

# 1 Atmospheric Isoprene Ozonolysis: Impacts of Stabilized 2 Criegee Intermediate Reactions with SO<sub>2</sub>, H<sub>2</sub>O and Dimethyl 3 sulfide

4  
5 **Mike J. Newland<sup>1,\*</sup>, Andrew R. Rickard<sup>2,3</sup>, Luc Vereecken<sup>4</sup>, Amalia Muñoz<sup>5</sup>,  
6 Milagros Ródenas<sup>5</sup>, William J. Bloss<sup>1</sup>**

7 [1]{University of Birmingham, School of Geography, Earth and Environmental Sciences,  
8 Birmingham, UK}

9 [\*]{now at: University of East Anglia, School of Environmental Sciences, Norwich, UK}

10 [2]{National Centre for Atmospheric Science (NCAS), University of York, York, UK}

11 [3]{Wolfson Atmospheric Chemistry Laboratories, Department of Chemistry, University of  
12 York, York, UK}

13 [4]{Max Planck Institute for Chemistry, Atmospheric Sciences, J.-J.-Becher-Weg 27, Mainz,  
14 Belgium}

15 [5]{Instituto Universitario CEAM-UMH, EUPHORE Laboratories, Avda/Charles R. Darwin.  
16 Parque Tecnológico, Valencia, Spain}

17 Correspondence to: W. J. Bloss ([W.J.Bloss@bham.ac.uk](mailto:W.J.Bloss@bham.ac.uk))

18 A. R. Rickard ([andrew.rickard@york.ac.uk](mailto:andrew.rickard@york.ac.uk))

## 19 20 **Abstract**

21 Isoprene is the dominant global biogenic volatile organic compound (VOC) emission.  
22 Reactions of isoprene with ozone are known to form stabilised Criegee intermediates (SCIs),  
23 which have recently been shown to be potentially important oxidants for SO<sub>2</sub> and NO<sub>2</sub> in the  
24 atmosphere; however the significance of this chemistry for SO<sub>2</sub> processing (affecting sulfate  
25 aerosol) and NO<sub>2</sub> processing (affecting NO<sub>x</sub> levels) depends critically upon the fate of the SCI  
26 with respect to reaction with water and decomposition. Here, we have investigated the  
27 removal of SO<sub>2</sub> in the presence of isoprene and ozone, as a function of humidity, under  
28 atmospheric boundary layer conditions. The SO<sub>2</sub> removal displays a clear dependence on

1 relative humidity, confirming a significant reaction for isoprene derived SCI with H<sub>2</sub>O. Under  
2 excess SO<sub>2</sub> conditions, the total isoprene ozonolysis SCI yield was calculated to be 0.56  
3 ( $\pm 0.03$ ). The observed SO<sub>2</sub> removal kinetics are consistent with a relative rate constant,  $k(\text{SCI}$   
4  $+ \text{H}_2\text{O}) / k(\text{SCI} + \text{SO}_2)$ , of  $3.1 (\pm 0.5) \times 10^{-5}$  for isoprene derived SCI. The relative rate  
5 constant for  $k(\text{SCI decomposition}) / k(\text{SCI} + \text{SO}_2)$  is  $3.0 (\pm 3.2) \times 10^{11} \text{ cm}^{-3}$ . Uncertainties are  
6  $\pm 2\sigma$  and represent combined systematic and precision components. These kinetic parameters  
7 are based on the simplification that a single SCI species is formed in isoprene ozonolysis, an  
8 approximation which describes the results well across the full range of experimental  
9 conditions. Our data indicate that isoprene-derived SCIs are unlikely to make a substantial  
10 contribution to gas-phase SO<sub>2</sub> oxidation in the troposphere. We also present results from an  
11 analogous set of experiments, which show a clear dependence of SO<sub>2</sub> removal in the isoprene-  
12 ozone system as a function of dimethyl sulfide concentration. We propose that this behaviour  
13 arises from a rapid reaction between isoprene-derived SCI and DMS; the observed SO<sub>2</sub>  
14 removal kinetics are consistent with a relative rate constant,  $k(\text{SCI} + \text{DMS}) / k(\text{SCI} + \text{SO}_2)$ , of  
15  $3.5 (\pm 1.8)$ . This result suggests that SCIs may contribute to the oxidation of DMS in the  
16 atmosphere and that this process could therefore influence new particle formation in regions  
17 impacted by emissions of unsaturated hydrocarbons and DMS.

18

## 19 **1 Introduction**

20 Atmospheric chemical processes exert a major influence on atmospheric composition.  
21 Identified gas-phase oxidants include the OH radical, ozone, NO<sub>3</sub> and under certain  
22 circumstances other species such as halogen atoms. Reactions with these oxidants can lead to  
23 (for example) chemical removal of primary air pollutants; formation of secondary pollutants  
24 (e.g. ozone, harmful to human and environmental health, and a greenhouse gas); and the  
25 transformation of gas-phase species to the condensed phase (e.g., SO<sub>2</sub> oxidation leading to the  
26 formation of sulfate aerosol, and the formation of functionalised organic compounds leading  
27 to secondary aerosol formation, which can influence radiation transfer and climate).

28 Stabilised Criegee intermediates (SCI), or carbonyl oxides, are formed in the atmosphere  
29 predominantly from the reaction of ozone with unsaturated hydrocarbons, though other  
30 processes may be important in certain conditions, e.g. alkyl iodide photolysis  
31 (Gravestock et al., 2010), dissociation of the DMSO peroxy radical (Asatryan and  
32 Bozzelli, 2008), and reactions of peroxy radicals with OH (Fittschen et al., 2014). SCI

1 have been shown in laboratory experiments and by theoretical calculations to oxidise SO<sub>2</sub>  
2 and NO<sub>2</sub> (e.g. Cox and Penkett, 1971; Welz et al., 2012; Taatjes et al., 2013; Ouyang et  
3 al., 2013; Stone et al., 2014) as well as a number of other trace gases found in the  
4 atmosphere. Recent field measurements in a boreal forest (Mauldin et al., 2012) and at a  
5 coastal site (Berresheim et al., 2014) have both identified an apparently missing process  
6 oxidising SO<sub>2</sub> to H<sub>2</sub>SO<sub>4</sub> (in addition to reaction with OH) and have implied SCI as a  
7 possible oxidant, acting alongside OH. Assessment of the importance of SCIs for  
8 tropospheric processing requires a quantitative understanding of their formation yields  
9 and atmospheric fate – in particular, the relative importance of bimolecular reactions (e.g.  
10 with SO<sub>2</sub>), unimolecular decomposition, and reaction with water vapour. Here we  
11 describe an experimental investigation into the formation and reactions of the SCIs  
12 derived from isoprene (the most abundant biogenic VOC), formed through the ozonolysis  
13 process, which dominates atmospheric SCI production, and studied under boundary layer  
14 conditions, to assess their potential contribution to tropospheric oxidation.

## 15 **1.1 Stabilised Criegee Intermediate Kinetics**

16 Ozonolysis derived CIs are formed with a broad internal energy distribution, yielding  
17 both chemically activated and stabilised CIs. SCIs can have sufficiently long lifetimes to  
18 undergo bimolecular reactions with H<sub>2</sub>O and SO<sub>2</sub>, amongst other species. Chemically  
19 activated CIs may undergo collisional stabilisation to an SCI (Scheme 1), or unimolecular  
20 decomposition or isomerisation.

21 To date the majority of studies have focused on the smallest SCI, CH<sub>2</sub>OO, because of the  
22 importance of understanding simple SCI systems (this species is formed in the ozonolysis of  
23 all terminal alkenes) and the ability to synthesize CH<sub>2</sub>OO from alkyl iodide photolysis, with  
24 sufficient yield to probe its kinetics. However, the unique structure of CH<sub>2</sub>OO (which  
25 prohibits isomerisation to a hydroperoxide intermediate) likely gives it a different reactivity  
26 and degradation mechanism to other SCI (Johnson and Marston, 2008).

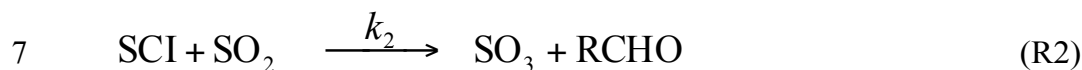
27 Recent experimental work (Berndt et al., 2014; Newland et al., 2015; Chao et al., 2015;  
28 Lewis et al., 2015) has determined the predominant atmospheric fate for CH<sub>2</sub>OO to be  
29 reaction with water vapour. Some of these experiments (Berndt et al., 2014; Chao et al.,  
30 2015; Lewis et al., 2015) have demonstrated a quadratic dependence of CH<sub>2</sub>OO loss on  
31 [H<sub>2</sub>O], suggesting a dominant role for the water dimer, (H<sub>2</sub>O)<sub>2</sub>, in CH<sub>2</sub>OO loss at typical

1 atmospheric boundary layer H<sub>2</sub>O concentrations. For larger SCI, both experimental  
2 (Taatjes et al., 2013; Sheps et al., 2014; Newland et al., 2015) and theoretical (Kuwata et  
3 al., 2010; Anglada et al., 2011) studies have shown that their kinetics, in particular  
4 reaction with water, are highly structure dependent. *syn*-SCI (*i.e.* those where an alkyl-  
5 substituent group is on the same side as the terminal oxygen of the carbonyl oxide  
6 moiety) react very slowly with H<sub>2</sub>O, whereas, *anti*-SCI (*i.e.* with the terminal oxygen of  
7 the carbonyl oxide moiety on the same side as a hydrogen group) react relatively fast  
8 with H<sub>2</sub>O. This difference has been predicted theoretically (Kuwata et al., 2010; Anglada  
9 et al., 2011) and was subsequently confirmed in recent experiments (Taatjes et al., 2013;  
10 Sheps et al., 2014) for the two CH<sub>3</sub>CHOO conformers. Additionally, it has been predicted  
11 theoretically (Vereecken et al., 2012) that the relative reaction rate constants for the water  
12 dimer vs water monomer,  $k(\text{SCI}+(\text{H}_2\text{O})_2)/k(\text{SCI}+\text{H}_2\text{O})$  of larger SCI (except *syn*-  
13 CH<sub>3</sub>CHOO) will be over 70 times smaller than that for CH<sub>2</sub>OO, suggesting that reaction  
14 with the water dimer is unlikely to be the dominant fate for these SCI under atmospheric  
15 conditions.

16 An additional, potentially important, fate of SCI under atmospheric conditions is  
17 unimolecular decomposition (denoted  $k_d$  in (R4)). This is likely to be a significant  
18 atmospheric sink for *syn*-SCI because of their slow reaction with water vapour. Previous  
19 studies have identified the hydroperoxide rearrangement as dominant for SCIs with a *syn*  
20 configuration, determining their overall unimolecular decomposition rate (Niki et al., 1987;  
21 Rickard et al., 1999; Martinez and Herron, 1987; Johnson and Marston, 2008). This route has  
22 been shown to be a substantial non-photolytic source of atmospheric oxidants (Niki et al.,  
23 1987; Alam et al., 2013). CIs formed in the *anti*-configuration are thought to primarily  
24 undergo rearrangement and possibly decomposition *via* a dioxirane intermediate (“the  
25 acid/ester channel”), producing a range of daughter products and contributing to the  
26 observed overall HO<sub>x</sub> radical yield (Johnson and Marston, 2008; Alam et al., 2013).

27 For CH<sub>2</sub>OO, rearrangement via a ‘hot’ acid species represents the lowest accessible  
28 decomposition channel with the theoretically predicted rate constant being rather low, 0.3 s<sup>-1</sup>  
29 (Olzmann et al., 1997). Recent experimental work supports this slow decomposition rate for  
30 CH<sub>2</sub>OO (Newland et al., 2015; Chhantyal-Pun et al., 2015). However, Newland *et al.* (2015)  
31 have suggested the decomposition of larger *syn*-SCI to be considerably faster, albeit with  
32 substantial uncertainty, with reported rate constants for *syn*-CH<sub>3</sub>CHOO of 288 (± 275) s<sup>-1</sup> and

1 for (CH<sub>3</sub>)<sub>2</sub>COO of 151 (± 35) s<sup>-1</sup>. Novelli *et al.* (2014), estimated decomposition of *syn*-  
2 CH<sub>3</sub>CHOO to be 20 (3-30) s<sup>-1</sup> from direct observation of OH formation, while Fenske *et al.*  
3 (2000), estimated decomposition of CH<sub>3</sub>CHOO produced from ozonolysis of *trans*-but-2-ene  
4 to be 76 s<sup>-1</sup> (accurate to within a factor of three).  
5



11

## 12 **1.2 Isoprene Ozonolysis**

13 Global emissions of biogenic VOCs have been estimated to be an order of magnitude greater,  
14 by mass, than anthropogenic VOC emissions (Guenther *et al.*, 1995). The most abundant non-  
15 methane biogenic hydrocarbon in the natural atmosphere is isoprene (2-methyl-1,3-butadiene,  
16 C<sub>5</sub>H<sub>8</sub>), with global emissions estimated to be 594 (± 34) Tg yr<sup>-1</sup> (Sindelarova *et al.*, 2014).  
17 While the vast majority of these emissions are from terrestrial sources, there are also biogenic  
18 emissions in coastal and remote marine environments, associated with seaweed and  
19 phytoplankton blooms (Moore *et al.*, 1994). Isoprene mixing ratios (as well as those of some  
20 monoterpenes) have been reported to reach hundreds of pptv (parts per trillion by volume)  
21 over active phytoplankton blooms in the marine boundary layer (Sinha *et al.*, 2007; Yassaa *et al.*,  
22 2008), with the potential to impact local air quality (Williams *et al.*, 2010).

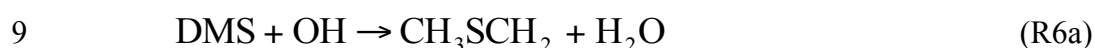
23 Removal of isoprene from the troposphere is dominated by reaction with the OH radical  
24 during the day and reaction with the nitrate radical during the night (Calvert *et al.*, 2000). The  
25 ozonolysis of isoprene is also a non-photolytic source of HO<sub>x</sub> radicals (Atkinson *et al.*, 1992;  
26 Paulson *et al.*, 1997; Malkin *et al.*, 2010), with measured yields of OH between 0.25 (Paulson  
27 *et al.*, 1997) and 0.27 (Atkinson *et al.*, 1992) (with a current recommended yield of 0.25  
28 (Atkinson *et al.*, 2006)). Isoprene ozonolysis also leads to the formation of a range of multi-  
29 functional oxygenated compounds, some of which can form secondary organic aerosol  
30 (Noziere *et al.*, 2015).

1 Isoprene ozonolysis yields five different initial carbonyl oxides (Scheme 2). The three basic  
2 species formed are formaldehyde oxide ( $\text{CH}_2\text{OO}$ ), methyl-vinyl carbonyl oxide (MVKOO)  
3 and methacrolein oxide (MACROO) (Calvert et al., 2000; Atkinson et al., 2006). MVKOO  
4 and MACROO both have *syn* and *anti* conformers and each of these can have either *cis* or  
5 *trans* configuration (Zhang et al., 2002; Kuwata et al., 2005) with easy inter-conversion  
6 between the *cis* and *trans* conformers (Aplincourt and Anglada, 2003). The kinetics and  
7 products of isoprene ozonolysis have been investigated theoretically by Zhang *et al.* (2002).  
8 They predicted the following SCI yields:  $\text{CH}_2\text{OO}$ , 0.31; *syn*-MVKOO, 0.14; *anti*-MVKOO,  
9 0.07; *syn*-MACROO, 0.01; *anti*-MACROO 0.04. This gives a total SCI yield of 0.57. They  
10 predicted that 95% of the chemically activated  $\text{CH}_2\text{OO}$  formed will be stabilized,  
11 considerably higher than the experimentally determined stabilization of excited  $\text{CH}_2\text{OO}$   
12 formed during ethene ozonolysis (35% - 54%) (Newland et al., 2015). This is because the  
13 majority of the energy formed during isoprene ozonolysis is thought to partition into the  
14 larger, co-generated, primary carbonyl species (Kuwata et al., 2005) (*i.e.* methyl-vinyl ketone  
15 (MVK) or methacrolein (MACR)). The predicted stabilization of the other SCI ranges from  
16 20% to 54% at atmospheric pressure. It is relevant to note that the total SCI yield from  
17 isoprene ozonolysis used in the Master Chemical Mechanism, MCMv3.2 (Jenkin et al., 1997,  
18 Saunders et al., 2003), is considerably lower at 0.22, as a consequence of the MCM protocol,  
19 which applies a weighted mean of total SCI yields measured for propene, 1-octene and 2-  
20 methyl propene (Jenkin et al., 1997). However, the relative yield of  $\text{CH}_2\text{OO}$  (0.50) compared  
21 to the total SCI yield in the MCM is very similar to that calculated by Zhang *et al.* (2002)  
22 (0.54).

### 23 **1.3 Dimethyl Sulfide (DMS)**

24 The largest natural source of sulfur to the atmosphere is the biogenically produced compound  
25 dimethyl sulfide, DMS ( $\text{CH}_3\text{SCH}_3$ ), which has estimated global emissions of 19.4 ( $\pm 4.4$ ) Tg  
26  $\text{yr}^{-1}$  (Faloona, 2009). DMS is a breakdown product of the plankton waste product  
27 dimethylsulfoniopropionate (DMSP). Jardine et al. (2015) have also recently shown that  
28 vegetation and soils can be important terrestrial sources of DMS to the atmosphere in the  
29 Amazon Basin, during both the day and at night, and throughout the wet and dry seasons,  
30 with measurements of up to 160 pptv within the canopy and near the surface. The oxidation of  
31 DMS is a large natural source of  $\text{SO}_2$ , and subsequently sulfate aerosol, to the atmosphere and  
32 therefore is an important source of new particle formation. This process has been implicated

1 in an important feedback leading to a regulation of the climate in the pre-industrial  
2 atmosphere (Charlson et al., 1987). The two most important oxidants of DMS in the  
3 atmosphere are thought to be the OH and NO<sub>3</sub> radicals (Barnes et al., 2006) (Reactions R6  
4 and R7). Because of its photochemical source, OH is thought to be the more important  
5 oxidant during the day in tropical regions, while NO<sub>3</sub> becomes more important at night, at  
6 high latitudes, and in more polluted air masses (Stark et al., 2007). Certain halogenated  
7 compounds, *e.g.* Cl (Wingenter et al., 2005) and BrO (Wingenter et al., 2005; Read et al.,  
8 2008), have also been suggested as possible oxidants for DMS in the marine environment.



12

## 13 **2 Experimental**

### 14 **2.1 Experimental Approach**

15 The EUPHORE facility is a 200 m<sup>3</sup> simulation chamber used primarily for studying reaction  
16 mechanisms under atmospheric boundary layer conditions. Further details of the chamber  
17 setup and instrumentation are available elsewhere (Becker, 1996; Alam et al., 2011), and a  
18 detailed account of the experimental procedure, summarised below, is given in Newland et al  
19 (2015).

20 Experiments comprised time-resolved measurement of the removal of SO<sub>2</sub> in the presence of  
21 the isoprene-ozone system, as a function of humidity or DMS concentration. SO<sub>2</sub> and O<sub>3</sub>  
22 abundance were measured using conventional fluorescence and UV absorption monitors,  
23 respectively; alkene abundance was determined via FTIR spectroscopy. Experiments were  
24 performed in the dark (*i.e.* with the chamber housing closed;  $j(\text{NO}_2) \leq 10^{-6} \text{ s}^{-1}$ ), at atmospheric  
25 pressure (*ca.* 1000 mbar) and temperatures between 287 and 302 K. The chamber is fitted  
26 with large horizontal and vertical fans to ensure rapid mixing (three minutes). Chamber  
27 dilution was monitored via the first order decay of an aliquot of SF<sub>6</sub>, added prior to each  
28 experiment. Cyclohexane (*ca.* 75 ppmv) was added at the beginning of each experiment to act

1 as an OH scavenger, such that SO<sub>2</sub> reaction with OH was calculated to be ≤ 1 % of the total  
2 chemical SO<sub>2</sub> removal in all experiments.

3 Experimental procedure, starting with the chamber filled with clean air, comprised addition of  
4 SF<sub>6</sub> and cyclohexane, followed by water vapour (or DMS), O<sub>3</sub> (*ca.* 500 ppbv) and SO<sub>2</sub> (*ca.* 50  
5 ppbv). A gap of five minutes was left prior to addition of isoprene, to allow complete mixing.  
6 The reaction was then initiated by addition of the isoprene (*ca.* 400 ppbv), and reagent  
7 concentrations followed for 30 -60 minutes; typically *ca.* 25% of the isoprene was consumed  
8 after this time. Nine isoprene + O<sub>3</sub> experiments, as a function of [H<sub>2</sub>O], were performed over  
9 separate days. Each individual run was performed at a constant humidity, with humidity  
10 varied to cover the range of [H<sub>2</sub>O] = 0.4–21 × 10<sup>16</sup> molecules cm<sup>-3</sup>, corresponding to an RH  
11 range of 0.5 – 27 % (at 298 K). Five isoprene + O<sub>3</sub> experiments as a function of DMS were  
12 also performed. Measured increases in [SO<sub>2</sub>] agreed with measured volumetric additions  
13 across the SO<sub>2</sub>, humidity and DMS ranges used in the experiments.

## 14 **2.2 Analysis**

15 As in our previous study (Newland et al., 2015), from the chemistry presented in Reactions  
16 R1 – R5 SCI will be produced in the chamber from the reaction of the alkene with ozone at a  
17 given yield,  $\phi$ . A range of different SCI are produced from the ozonolysis of isoprene (see  
18 Scheme 2: 9 first-generation SCI present), each with their own distinct chemical behaviour  
19 (*i.e.* yields, reaction rates). It is not feasible (from these experiments) to obtain data for each  
20 SCI independently, consequently for analytical purposes we adopt two alternative analyses to  
21 treat the SCI population in a simplified (lumped) manner:

22 In the first of these, we make the approximation that all SCI may be considered as a single  
23 species (defined from now on as ISOP-SCI). Alternatively, the SCI population is grouped into  
24 two species, the first of which is CH<sub>2</sub>OO (for which the kinetics are known) and the second  
25 (hereafter termed CRB-SCI) represents all isomers of the other SCI species produced, *i.e.*  
26  $\Sigma(\text{MVKOO} + \text{MACROO})$ . The implications of these assumptions are discussed further  
27 below, but a key consequence is that the relative rate constants obtained from the analysis  
28 presented here are not representative of the elementary reactions of any single specific SCI  
29 isomer formed, but rather represent a quantitative ensemble description of the integrated  
30 system, under atmospheric boundary layer conditions, which may be appropriate for  
31 atmospheric modelling.



1 Following formation in the ozonolysis reaction, the SCI can react with SO<sub>2</sub>, with H<sub>2</sub>O, with  
 2 DMS (if present), with other species, or undergo unimolecular decomposition, under the  
 3 experimental conditions applied. The fraction of the SCI produced that reacts with SO<sub>2</sub> ( $f$ ) is  
 4 determined by the SO<sub>2</sub> loss rate ( $k_2[\text{SO}_2]$ ) compared to the sum of the total loss processes of  
 5 the SCI (Equation E1) :

$$6 \quad f = \frac{k_2[\text{SO}_2]}{k_2[\text{SO}_2] + k_3[\text{H}_2\text{O}] + k_d + L} \quad (\text{E1})$$

7 Here,  $L$  accounts for the sum of any other chemical loss processes for SCI in the chamber,  
 8 after correction for dilution, and neglecting other (non-alkene) chemical sinks for O<sub>3</sub>, such as  
 9 reaction with HO<sub>2</sub> (also produced directly during alkene ozonolysis (Alam et al., 2013;  
 10 Malkin et al., 2010)), which was indicated through model calculations to account for < 0.5 %  
 11 of ozone loss under all the experimental conditions.

### 12 2.2.1 SCI yield calculation

13 The value for the total SCI yield of ISOP-SCI,  $\phi_{\text{ISOP-SCI}}$ , was determined from an experiment  
 14 performed under dry conditions (RH < 1%) in the presence of excess SO<sub>2</sub> (*ca.* 1000 ppbv),  
 15 such that SO<sub>2</sub> scavenged the majority of the SCI (>95%). From Equation E2, regressing  $d\text{SO}_2$   
 16 against  $d\text{O}_3$  (corrected for chamber dilution), assuming  $f$  to be unity (*i.e.* all the SCI produced  
 17 reacts with SO<sub>2</sub>), determines the value of  $\phi_{\text{min}}$ , a lower limit to the SCI yield. Figure 1 shows  
 18 the experimental data, from which  $\phi_{\text{min}}$  was derived.

$$19 \quad \frac{d[\text{SO}_2]}{d[\text{O}_3]} = \varphi \cdot f \quad (\text{E2})$$

20 The lower limit criterion applies as in reality  $f$  will be less than one, at experimentally  
 21 accessible SO<sub>2</sub> levels, as a small fraction of the SCI will still react with trace H<sub>2</sub>O present, or  
 22 undergo decomposition. The actual yield,  $\phi_{\text{ISOP-SCI}}$ , was determined by combining the result  
 23 from the excess-SO<sub>2</sub> experiment with those from the series of experiments performed at lower  
 24 SO<sub>2</sub>, as a function of [H<sub>2</sub>O], to determine  $k_3/k_2$  and  $k_d/k_2$  (see Section 2.2.2), through an  
 25 iterative process to determine the single unique value of  $\phi_{\text{ISOP-SCI}}$  which fits both datasets.

### 1 2.2.2 $k(\text{SCI}+\text{H}_2\text{O})/k(\text{SCI}+\text{SO}_2)$ and $k_d/k(\text{SCI}+\text{SO}_2)$

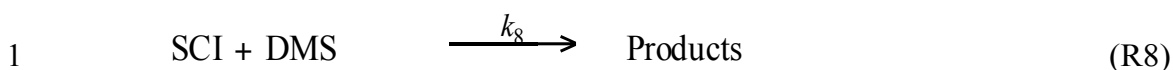
2 By rearranging Equation E1, the following equation (E3) can be derived. Therefore, in order  
3 to determine the relative rate constants  $k_3/k_2$  and  $(k_d+L)/k_2$ , a series of experiments were  
4 performed in which the  $\text{SO}_2$  loss was monitored as a function of  $[\text{H}_2\text{O}]$  (see Section 2.1).

$$6 \quad [\text{SO}_2] \left( \frac{1}{f} - 1 \right) = \frac{k_3}{k_2} [\text{H}_2\text{O}] + \frac{k_d + L}{k_2} \quad (\text{E3})$$

7  
8 From Equation E2, regression of the loss of ozone ( $d\text{O}_3$ ) against the loss of  $\text{SO}_2$  ( $d\text{SO}_2$ ) for an  
9 experiment at a given RH determines the product  $f \cdot \phi$  at a given point in time. This quantity  
10 will vary through the experiment as  $\text{SO}_2$  is consumed, and other potential SCI co-reactants are  
11 produced, as predicted by Equation E1. A smoothed fit was applied to the experimental data  
12 for the cumulative consumption of  $\text{SO}_2$  and  $\text{O}_3$ ,  $\Delta\text{SO}_2$  and  $\Delta\text{O}_3$ , (as shown in Figure 2) to  
13 determine  $d\text{SO}_2/d\text{O}_3$  (and hence  $f \cdot \phi$ ) at the start of each experiment, for use in Equation E3.  
14 This fit was derived using a box model run in FACSIMILE (Curtis and Sweetenham, 1987)  
15 with a chemical scheme taken from MCM, v3.2 (<http://mcm.leeds.ac.uk/MCM>), with  
16 additional updated SCI chemistry constrained by the experimental measurements. The start of  
17 each experiment (*i.e.* when  $[\text{SO}_2] \sim 50$  ppbv) was used as this corresponds to the greatest rate  
18 of production of the SCI, and hence largest experimental signals (*i.e.*  $\text{O}_3$  and  $\text{SO}_2$  rate of  
19 change; greatest precision) and is the point at which the SCI +  $\text{SO}_2$  reaction has the greatest  
20 magnitude compared with any other potential loss processes for either reactant species (see  
21 discussion below). The value  $[\text{SO}_2]((1/f) - 1)$  can then be regressed against  $[\text{H}_2\text{O}]$  for each  
22 experiment to give a plot with a gradient of  $k_3/k_2$  and an intercept of  $(k_d + L)/k_2$  (Equation E3).  
23 Our data cannot determine absolute rate constants (*i.e.* values of  $k_2$ ,  $k_3$ ,  $k_d$ ) in isolation, but is  
24 limited to assessing their relative values, which may be placed on an absolute basis through  
25 use of an (external) reference value ( $k_2(\text{CH}_2\text{OO} + \text{SO}_2)$  in this case).

### 26 2.2.3 $k(\text{SCI}+\text{DMS})/k(\text{SCI}+\text{SO}_2)$

27 A similar methodology was applied to that detailed in Section 2.2.2 to determine the relative  
28 reaction rate of ISOP-SCI with DMS  $k(\text{SCI}+\text{DMS})/k(\text{SCI}+\text{SO}_2)$ ,  $k_8/k_2$ . Here, the  $\text{SO}_2$  loss was  
29 determined as a function of  $[\text{DMS}]$  rather than  $[\text{H}_2\text{O}]$ .  $[\text{H}_2\text{O}]$  was  $< 1 \times 10^{16}$  molecules  $\text{cm}^{-3}$   
30 for all experiments.



2 Equation E3 is modified to give Equation E4 by the addition of the DMS term. The gradient  
 3 of a plot regressing  $[\text{SO}_2](\frac{1}{f} - 1)$  against  $[\text{DMS}]$  is then  $k_8/k_2$  and the intercept is  $k_3/k_2[\text{H}_2\text{O}]$   
 4  $+ (k_d + L)/k_2$ . Using this intercept, these experiments can also be used to validate the  $k_3/k_2$  and  
 5  $(k_d + L)/k_2$  values derived from the experiments described in Section 2.2.

$$6 \quad [\text{SO}_2] \left( \frac{1}{f} - 1 \right) = \frac{k_8}{k_2} [\text{DMS}] + \frac{k_3}{k_2} [\text{H}_2\text{O}] + \frac{k_d + L}{k_2} \quad (\text{E4})$$

7

### 8 **3 Isoprene + Ozone as a function of $[\text{H}_2\text{O}]$**

#### 9 **3.1 SCI Yield**

10 Figure 1 shows the derived  $\phi_{\text{min}}$  for isoprene, 0.55, determined from fitting Equation E2 to the  
 11 experimental data.  $\phi_{\text{min}}$  was then corrected ( $< 3\%$ ) as described in Section 2.2.1 using the  
 12  $k_3/k_2$  and  $k_d/k_2$  values determined from the measurements shown in Figure 3 using Equation  
 13 E5. The corrected yield,  $\phi_{\text{ISOP-SCI}}$ , is 0.56 ( $\pm 0.03$ ). Uncertainties are  $\pm 2\sigma$ , and represent the  
 14 combined systematic (estimated measurement uncertainty) and precision components.

15 Literature yields for SCI production from isoprene ozonolysis are given in Table 1. The value  
 16 derived for the yield in this work agrees very well with the value of 0.58 ( $\pm 0.26$ ) from a  
 17 recent experimental study (Sipilä et al., 2014) which used a similar single-SCI analysis  
 18 approach.

19 Earlier experimental studies have reported lower values (by up to a factor of 2) for the total  
 20 isoprene SCI yield. Rickard *et al.* (1999) derive a total yield of 0.28 from the increase in  
 21 primary carbonyl yield (MVK and MACR) in the presence of a suitable SCI scavenger  
 22 (excess  $\text{SO}_2$ ). However, owing to the fact that they could not measure a formaldehyde yield,  
 23 in their analysis it was assumed that 40 % of the chemically activated  $\text{CH}_2\text{OO}$  formed was  
 24 stabilised (derived from the measured  $\text{CH}_2\text{OO}$  SCI yield for ethene ozonolysis),  
 25 corresponding to their determination of a  $\text{CH}_2\text{OO}$  SCI yield of 0.18 for isoprene ozonolysis. If  
 26 it is assumed that 95% of the  $\text{CH}_2\text{OO}$  formed was actually stabilised, as calculated by Zhang  
 27 *et al.* (2002), then this yield increases to 0.43, giving a total yield,  $\phi_{\text{ISOP-SCI}}$ , of 0.53, in  
 28 excellent agreement with the current work. Hasson et al. (2001) calculated a total SCI yield of

1 0.26 by measuring the sum of the difference between (i) the H<sub>2</sub>O<sub>2</sub> production under dry and  
2 high RH conditions (to give the non-CH<sub>2</sub>OO SCI yield) and (ii) the difference between  
3 hydroxyl-methyl hydroperoxide (HMHP) production under dry and high RH conditions (to  
4 give  $\phi_{\text{CH}_2\text{OO}}$ ). One potential reason for the significantly lower total SCI calculated by Hasson  
5 et al. compared to this work is the low value of  $\phi_{\text{CH}_2\text{OO}}$  determined, potentially due to HMHP  
6 losses. Neeb et al. (1997) determined a value for  $\phi_{\text{CH}_2\text{OO}}$  approximately twice that determined  
7 by Hasson et al., using a similar methodology. This discrepancy may be owing to the fact that  
8 Hasson et al. do not account for the formation of formic acid, which is a degradation product  
9 of HMHP. From theoretical calculations, Zhang *et al.* (2002) predicted a yield of 0.31 for  
10 CH<sub>2</sub>OO, the most basic SCI, 0.14 for *syn*-MVKOO, 0.07 for *anti*-MVKOO, 0.04 for *anti*-  
11 MACROO and 0.01 for *syn*-MACROO. This gives a sum of SCI yields of 0.57, again in very  
12 good agreement with the overall value derived here. The MCM (Jenkin et al., 1997; Saunders  
13 et al., 2003) applies a  $\phi_{\text{ISOP-SCI}}$  of 0.22, based on the limited experimental data available at the  
14 time of its original release (Jenkin et al., 1997). Although this total value is slightly lower than  
15 the experimental measurements reported prior to the release of MCMv3.2 (i.e. Rickard et al.  
16 (1999) and Hasson et al. (2001)), the protocol uses a similar relative yield for stabilised-  
17 CH<sub>2</sub>OO (0.50) compared to the total SCI yield as reported by Zhang et al. (2002). A probable  
18 reason for the low SCI yields in the MCM is the assumption of low stabilisation of the  
19 chemically activated CI formed.

20 The CH<sub>2</sub>OO yield ( $\phi_{\text{CH}_2\text{OO}}$ ) from isoprene ozonolysis derived in this work can be calculated  
21 by multiplying the total SCI yield (0.56) by the fraction of the total SCI yield predicted to be  
22 CH<sub>2</sub>OO by Zhang *et al.* (2002) (0.54). This gives a yield of stabilised CH<sub>2</sub>OO from this work  
23 of 0.30. This is in very good agreement with Neeb *et al.* (1997) who derived a yield of  
24 stabilised CH<sub>2</sub>OO from isoprene ozonolysis of 0.30 by measuring hydroxymethyl  
25 hydroperoxide formation (HMHP, the product of CH<sub>2</sub>OO + H<sub>2</sub>O).

### 26 **3.2 Analysis 1: Single SCI (ISOP-SCI) treatment**

27 Figure 2 shows the cumulative consumption of SO<sub>2</sub> relative to that of O<sub>3</sub>,  $\Delta\text{SO}_2$  versus  $\Delta\text{O}_3$   
28 (after correction for dilution), for each isoprene ozonolysis experiment as a function of [H<sub>2</sub>O].  
29 A fit to each experiment, which has the sole purpose of extrapolating the experimental data to  
30 evaluate  $d\text{SO}_2/d\text{O}_3$  at  $t = 0$  (start of each experimental run) for use in Equations E1 - E3, is  
31 also shown. This fit is derived using a box model run in FACSIMILE (Curtis and

1 Sweetenham, 1987) as described in Section 2.2.2. The overall change in SO<sub>2</sub>, ΔSO<sub>2</sub>, is seen to  
2 decrease substantially with increasing humidity over a relatively narrow range of [H<sub>2</sub>O] (0.4 –  
3 21 × 10<sup>16</sup> cm<sup>-3</sup>). This trend is similar to that seen for smaller, structurally less complex alkene  
4 ozonolysis systems (Newland et al., 2015), and is as would be expected from the understood  
5 chemistry (R1 – R5), as there is competition between SO<sub>2</sub>, H<sub>2</sub>O, and decomposition for  
6 reaction with the SCI formed.

7 Other potential fates for SCIs under the experimental conditions presented here include  
8 reaction with other reactants / co-products: ozone (Kjaergaard et al., 2013; Vereecken et al.,  
9 2014; Wei et al., 2014), other SCI (Su et al., 2014; Vereecken et al., 2014), carbonyl products  
10 (Taatjes et al., 2012), acids (Welz et al., 2014), or the parent alkene itself (Vereecken et al.,  
11 2014). Sensitivity analyses were performed using a box model run in FACSIMILE (Curtis  
12 and Sweetenham, 1987) with a chemical scheme taken from the MCM, with additional  
13 updated SCI chemistry. Based on reported reaction rates of ozonolysis products with SCIs,  
14 these analyses indicate that the only reaction partners likely to compete significantly with  
15 SO<sub>2</sub>, H<sub>2</sub>O or unimolecular decomposition under the experimental conditions applied here are  
16 organic acids (i.e. HCOOH and CH<sub>3</sub>COOH); these formed during the experiments, at  
17 concentrations reaching up to 2.5 × 10<sup>12</sup> cm<sup>-3</sup>. All other potential co-reactants listed above  
18 were calculated to account for < 10 % (for the worst case run) of the total SCI loss under the  
19 experimental conditions applied.

20 Model runs were performed in which a rate constant of 1.1 × 10<sup>-10</sup> cm<sup>3</sup> s<sup>-1</sup> was used for  
21 reaction between SCI and formic and acetic acids (HCOOH, CH<sub>3</sub>COOH), as given by Welz et  
22 al. (2014) for CH<sub>2</sub>OO + HCOOH, together with an acid yield of 0.5 from the reactions of  
23 isoprene derived SCI species with water, which gave a good agreement with the  
24 experimentally determined acid yields measured by FTIR. The reduction in SO<sub>2</sub> loss between  
25 the model runs with the SCI + acid reaction included, and those without the reaction, varied  
26 between 7 % and 17 %.

27 Equation E3 can be extended to explicitly account for the presence of acids by inclusion of a  
28 further term (Equation E5). This requires a value for  $k_9/k_2$ , the ratio of the rate constants for  
29 SCI reactions with acids and with SO<sub>2</sub>. Here, we employ a value of 3.0, derived from the  
30 mean of the recently reported rates of reaction of CH<sub>2</sub>OO with HCOOH and CH<sub>3</sub>COOH  
31 (Welz et al., 2014), and the rate constant for CH<sub>2</sub>OO + SO<sub>2</sub> reported by Welz et al. (2012) –

1 although in reality this term represents potential reaction of all SCI present with multiple acid  
 2 species. The acid concentrations are taken from FTIR measurements during the experiments.



$$4 \quad [\text{SO}_2] \left( \frac{1}{f} - 1 \right) - \frac{k_9}{k_2} [\text{Acid}] = \frac{k_3}{k_2} [\text{H}_2\text{O}] + \frac{k_d + L}{k_2} \quad (\text{E5})$$

5 Figure 3 shows a fit of Equation E5 to the data shown in Figure 2, giving a gradient of  $k_3/k_2$ ,  
 6 and an intercept of the (relative) rate of SCI decomposition  $(k_d + L)/k_2$ . The results are well  
 7 described by the linear relationship (E5) across the full range of experimental conditions. This  
 8 suggests that the analytical approach described – of treating the SCI produced from isoprene  
 9 ozonolysis as a single system – provides a good quantitative description of the ISO-  
 10 SCI/O<sub>3</sub>/H<sub>2</sub>O/SO<sub>2</sub> system under atmospheric boundary layer conditions, and hence provides a  
 11 good approximation for use in atmospheric modelling studies. Reaction with the water dimer  
 12 is not considered in this analysis (see discussion below). From Figure 3 it is apparent that the  
 13 observations can be described well by a linear dependence on [H<sub>2</sub>O] across the full range of  
 14 experimental conditions applied. However, the humidity levels accessible in these  
 15 experiments were limited (constrained by the operational range of the FTIR retrievals), and  
 16 [H<sub>2</sub>O] can range up to  $\sim 1 \times 10^{18} \text{ cm}^{-3}$  in the atmosphere; the derived relationship may work  
 17 less well at these high RH as the role of the water dimer becomes more important; this is  
 18 considered further in Section 3.3 (below) in which the SCI mix formed during isoprene  
 19 ozonolysis is separated into CH<sub>2</sub>OO and the other SCI formed.

20 From Figure 3, the derived relative rate constant for reaction of ISOP-SCI with water vs. SO<sub>2</sub>,  
 21  $k_3/k_2$ , is  $3.1 (\pm 0.5) \times 10^{-5}$  (Table 2). Newland et al. (2015) recently reported a  $k_3/k_2$  relative  
 22 rate constant for CH<sub>2</sub>OO of  $3.3 (\pm 1.1) \times 10^{-5}$  using the same experimental approach as used  
 23 in this study. The value derived for ISOP-SCI here is the same, within uncertainty, as that  
 24 derived for CH<sub>2</sub>OO, suggesting that the other SCI formed during isoprene ozonolysis have a  
 25 mean  $k_3/k_2$  similar to that of CH<sub>2</sub>OO.

26 No absolute values of  $k_2$  (SCI+SO<sub>2</sub>) have been measured for ISOP-SCI. However Welz et al.  
 27 (2012) obtained an absolute value of  $k_2$  (298 K) for CH<sub>2</sub>OO ( $3.9 \times 10^{-11} \text{ cm}^3 \text{ s}^{-1}$ ), using direct  
 28 methods at reduced pressure (a few Torr). If this value is used as an approximation for the  $k_2$   
 29 value of ISOP-SCI (at atmospheric pressure and ambient temperature), then a  $k_3$  (ISOP-SCI +

1 H<sub>2</sub>O) value of  $1.2 (\pm 0.2) \times 10^{-15} \text{ cm}^3 \text{ s}^{-1}$  is determined (assuming the reaction between ISOP-  
2 SCI and water vapour is dominated by reaction with the water monomer, rather than the  
3 dimer, as discussed above).

4 From Equation E5, the intercept in Figure 3 gives the term  $(k_d + L)/k_2$ .  $(k_d + L)$  will be  
5 dominated by  $k_d$  under the experimental conditions applied and analysis extrapolation to the  
6 start of each experimental run; however, the possibility of other chemical loss processes (see  
7 below) dictates that the derived value for  $k_d$  is technically an upper limit. From Figure 3,  $k_d/k_2$   
8 is determined to be  $3.0 (\pm 3.2) \times 10^{11} \text{ cm}^{-3}$  (Table 2). Using the  $k_2$  value determined by Welz  
9 et al. (2012) to put  $k_d/k_2$  on an absolute scale (as above for  $k_3$ ) yields a  $k_d$  of  $\leq 12 (\pm 12) \text{ s}^{-1}$ .  
10 Newland et al. (2015) recently determined  $k_d$  for CH<sub>2</sub>OO to be  $\leq 4.7 \text{ s}^{-1}$ . This suggests that  
11 either  $k_d$  for the non-CH<sub>2</sub>OO SCI within the ISOP-SCI family is relatively low, *i.e.* a few tens  
12  $\text{s}^{-1}$ , and/or that CH<sub>2</sub>OO dominates the ISOP-SCI population. The limited precision obtained  
13 for these  $k_d$  values reflects the uncertainty in the intercept of the regression analysis shown in  
14 Figure 3.

15 Sipilä et al. (2014) recently reported a value of  $k_{loss}/k_2$  for isoprene ozonolysis derived SCI,  
16 treated using a single-SCI approach, which is analogous to the value  $(k_3[\text{H}_2\text{O}] + k_d)/k_2$   
17 reported in this section. They derive a value of  $2.5 (\pm 0.1) \times 10^{12} \text{ cm}^{-3}$  at  $[\text{H}_2\text{O}] = 5.8 \times 10^{16}$   
18  $\text{cm}^{-3}$ . From the  $k_3$  and  $k_d$  values derived in the single SCI analysis in this work (Table 2) we  
19 calculate a value of  $2.1 (\pm 0.6) \times 10^{12} \text{ cm}^{-3}$  at the same  $[\text{H}_2\text{O}]$ , in good agreement.

20 The results presented here suggest that while SCI and conformer specific identification is  
21 important to determine the product yields, it does not appear to be important when solely  
22 considering the combined effects of isoprene ozonolysis products on the oxidation of SO<sub>2</sub>  
23 under the experimental conditions applied.

### 24 **3.3 Analysis 2: Two-SCI species (CH<sub>2</sub>OO + CRB-SCI) treatment**

25 In the preceding section, the combined effects of the five SCI initially produced during  
26 isoprene ozonolysis were treated as a single pseudo-SCI, ISOP-SCI. In this section an  
27 alternative approach is presented, in which the SCI family is split into two components. These  
28 are: CH<sub>2</sub>OO, for which the reaction rates with water and the water dimer have been quantified  
29 in recent experimental studies, and the sum of the MVKOO and MACROO SCI, denoted  
30 CRB-SCI.

1 To date, the effects of the water dimer, (H<sub>2</sub>O)<sub>2</sub> have only been determined experimentally for  
 2 CH<sub>2</sub>OO (Berndt et al., 2014; Chao et al., 2015; Lewis et al., 2015; Newland et al., 2015).  
 3 Theoretical calculations (Vereecken et al., 2012) predicted the significant effect of the water  
 4 dimer compared to the monomer for CH<sub>2</sub>OO, but also that the ratio of the SCI + (H<sub>2</sub>O)<sub>2</sub> : SCI  
 5 + H<sub>2</sub>O rate constants,  $k_5/k_3$ , of the larger, more substituted SCI, *anti*-CH<sub>3</sub>CHOO and  
 6 (CH<sub>3</sub>)<sub>2</sub>COO, are 2 - 3 orders of magnitude smaller than for CH<sub>2</sub>OO (Vereecken et al., 2012).  
 7 This would make the dimer reaction negligible at atmospherically accessible [H<sub>2</sub>O] (*i.e.* < 1 ×  
 8 10<sup>18</sup> cm<sup>-3</sup>) for SCI larger than CH<sub>2</sub>OO. The results presented in Section 3.2 show that, under  
 9 the single-SCI treatment of the isoprene ozonolysis SCI chemistry, a water monomer only  
 10 approach is able to describe the experimental data. Hence the effect of the water dimer  
 11 reaction on CRB-SCI is not considered in this analysis (the water dimer reaction is included  
 12 for CH<sub>2</sub>OO).

$$13 \quad [\text{SO}_2] \left( \frac{1}{f} - 1 \right) - \frac{k_9}{k_2} [\text{Acid}] = \gamma^A \left( \frac{k_3^A [\text{H}_2\text{O}] + k_5^A [(\text{H}_2\text{O})_2] + (k_d^A + L^A)}{k_2^A} \right) + \gamma^C \left( \frac{k_3^C [\text{H}_2\text{O}] + (k_d^C + L^C)}{k_2^A} \right) \quad (\text{E6})$$

14 where <sup>A</sup> denotes CH<sub>2</sub>OO and <sup>C</sup> denotes CRB-SCI.

15 Figure 4 shows three fits, obtained using Equation E6 and corresponding to different  
 16 treatments for the reaction of CH<sub>2</sub>OO with H<sub>2</sub>O and with (H<sub>2</sub>O)<sub>2</sub>, to the measured data  
 17 presented in Figure 3. For all three scenarios, the relative contribution of the two SCI  
 18 components to the total SCI yield ( $\gamma$ ) was assumed to be  $\gamma^A = 0.54$  and  $\gamma^C = 0.46$ , after Zhang  
 19 *et al.* (2002).  $k_3^A/k_2^A$  is assumed to be  $3.3 \times 10^{-5}$  after Newland *et al.* (2015).

20 The solid red line in Figure 4 is a linear fit to the data to determine  $k_3^C$  and  $k_d^C$ . The CH<sub>2</sub>OO +  
 21 (H<sub>2</sub>O)<sub>2</sub> rate constant,  $k_5^A$ , was assumed to be zero to reduce the number of free parameters.  
 22 This assumption is reasonable considering the apparent linear dependence of the presented  
 23 measurements on [H<sub>2</sub>O] across the full range of conditions applied. The linear fit determines a  
 24 value of  $k_3^C/k_2^A = 2.9 (\pm 0.7) \times 10^{-5}$  and a value of  $(k_d^C + L^C)/k_2^A$  (CRB-SCI) =  $6.6 (\pm 7.0) \times$   
 25  $10^{11} \text{ cm}^{-3}$  (Table 2). Again, as for the single species analysis, the decomposition term is poorly  
 26 constrained.

27 The dashed blue line fits Equation E6 using the parameters derived above for CRB-SCI and  
 28 the water dimer relative reaction rate for CH<sub>2</sub>OO determined in Newland *et al.* (2015),  $k_5/k_2 =$   
 29  $0.014 (\pm 0.018)$ . This still gives a good fit to the data in Figure 4. The dotted green line is a  
 30 similar fit but uses the recently directly determined CH<sub>2</sub>OO + (H<sub>2</sub>O)<sub>2</sub> rate,  $k_5^A$ , of  $6.5 (\pm 0.8)$



1  $\times 10^{-12} \text{ cm}^3 \text{ s}^{-1}$  by Chao *et al.* (2015). It is seen that this fit considerably overestimates the  
2 observations at higher  $[\text{H}_2\text{O}]$ . However, owing to the quadratic relationship of  $[(\text{H}_2\text{O})_2]$  to  
3  $[\text{H}_2\text{O}]$  a small difference in the rate constant can have a large effect, especially at higher  
4  $[\text{H}_2\text{O}]$ . Possible explanations for this discrepancy are: (i) that the kinetics observed for  
5  $\text{CH}_2\text{OO}$  as formed from  $\text{CH}_2\text{I}_2$  photolysis are not representative of the behaviour of the  
6  $\text{CH}_2\text{OO}$  moiety as formed through alkene ozonolysis (although the conditions are such that a  
7 thermalized population would be expected in both cases); (ii) that the fraction of the total  
8 isoprene SCI yield that is  $\text{CH}_2\text{OO}$  is lower than that predicted by Zhang *et al.* (2002), hence  
9 the effect of the  $(\text{H}_2\text{O})_2$  reaction overall is reduced – however, the predicted yield is in good  
10 agreement with those determined experimentally, albeit using indirect methods, so it seems  
11 unlikely that the actual  $\text{CH}_2\text{OO}$  yield is considerably lower; (iii) multiple effects are affecting  
12 the curvature of the results shown in Figure 4. Analogous plots for  $\text{CH}_3\text{CHOO}$  shown in  
13 Newland *et al.* (2015) displayed a shallowing gradient with increasing  $[\text{H}_2\text{O}]$  (*i.e.* the opposite  
14 curvature to that caused by the  $(\text{H}_2\text{O})_2$  reaction). The probable explanation for the curvature  
15 observed for  $\text{CH}_3\text{CHOO}$  is the presence of a mix of *syn* and *anti* conformers (Scheme 2) in  
16 the system and the competing effects of the different kinetics of these two distinct forms of  
17  $\text{CH}_3\text{CHOO}$ . A similar effect may arise for the isoprene derived CRB-SCI which include  
18 multiple *syn* and *anti* conformers (see Scheme 2). The competition of this effect with that  
19 expected from the water dimer reaction may effectively lead to one masking the other under  
20 the experimental conditions applied.

21 Rate data for the reactions of isoprene derived SCI obtained using both analytical approaches  
22 described are given in Table 2.

### 23 **3.4 Atmospheric Implications**

24 Treatment of the SCI produced from isoprene ozonolysis as a single SCI system appears to  
25 describe the observations well over the full range of experimental conditions accessible in this  
26 work (Section 3.2). The derived values for  $k_3(\text{ISOP-SCI})$  reported here, obtained by fitting  
27 Equation E5 to the measurements, placed on an absolute basis using the measured  $k_2(\text{CH}_2\text{OO}$   
28  $+\text{SO}_2)$  of  $3.9 \times 10^{-11} \text{ cm}^3 \text{ s}^{-1}$  (Welz *et al.*, 2012)), corresponds to a loss rate for ISOP-SCI  
29 from reaction with  $\text{H}_2\text{O}$  in the atmosphere of  $340 \text{ s}^{-1}$  (assuming  $[\text{H}_2\text{O}] = 2.8 \times 10^{17} \text{ molecules}$   
30  $\text{cm}^{-3}$ , equivalent to an RH of 65 % at 288 K). Comparing this to the derived  $k_d$  value,  $12 (\pm 12)$   
31  $\text{s}^{-1}$ , it is seen that reaction with  $\text{H}_2\text{O}$  is predicted to be the main sink for isoprene derived SCI

1 in the atmosphere, with other sinks, such as decomposition and other bimolecular reactions,  
2 being negligible. Hence  $k_d$  is neglected in the following analysis.

3 An estimate of a mean steady state ISOP-SCI concentration in the background atmospheric  
4 boundary layer can be calculated using Equation E7.

$$5 \quad [ISOP - SCI]_{ss} = \frac{[Isoprene][O_3]k_1\phi}{k_3[H_2O]} \quad (E7)$$

6 Using the data given below, a steady state SCI concentration of  $4.1 \times 10^2$  molecules  $cm^{-3}$  is  
7 calculated for an isoprene ozonolysis source. This assumes an ozone mixing ratio of 40 ppbv,  
8 an isoprene mixing ratio of 1 ppbv, an SCI yield  $\phi$  of 0.56, and a reaction rate constant  $k_1$   
9 (isoprene – ozone) of  $1.0 \times 10^{-17}$   $cm^3 s^{-1}$  (288 K) (Atkinson et al., 2006);  $k_2$  (ISOP-SCI + SO<sub>2</sub>)  
10 of  $3.9 \times 10^{-11}$   $cm^3 s^{-1}$ ,  $k_3$  (ISOP-SCI + H<sub>2</sub>O) of  $1.2 \times 10^{-15}$   $cm^3 s^{-1}$  with [H<sub>2</sub>O] of  $2.8 \times 10^{17}$   $cm^{-3}$   
11 (RH ~ 65 % at 288 K). A typical diurnal loss rate of SO<sub>2</sub> to OH ( $k_{OH}[OH]$ ) is  $9 \times 10^{-7}$   $s^{-1}$   
12 (Welz et al., 2012), while the SO<sub>2</sub> loss rate arising from reaction with ISOP-SCI, using the  
13 values above, would be  $1.6 \times 10^{-8}$   $s^{-1}$ . This suggests, for the conditions given above, the  
14 diurnally averaged loss of SO<sub>2</sub> to SCI to be a very small fraction (1 – 2 %) of that due to OH.  
15 This analysis neglects additional chemical sinks for SCI, which would reduce SCI abundance,  
16 and the possibility of other alkene ozonolysis products leading to SO<sub>2</sub> oxidation which may  
17 increase the impact of alkene ozonolysis upon gas-phase SO<sub>2</sub> processing (Mauldin et al.,  
18 2012; Curci et al., 1995; Prousek, 2009). However, the analysis also neglects additional  
19 sources of SCI, e.g. photolysis of alkyl iodides (Gravestock et al., 2010; Stone et al., 2013),  
20 dissociation of the dimethyl sulfoxide (DMSO) peroxy radical (Asatryan and Bozzelli, 2008;  
21 Taatjes et al., 2008), and reactions of peroxy radicals with OH (Fittschen et al., 2014), which  
22 are currently poorly constrained and may even dominate SCI production over an ozonolysis  
23 source in some environments.

24 SCI concentrations are expected to vary greatly depending on the local environment, e.g.  
25 alkene abundance may be considerably higher (and with a different reactive mix of alkenes  
26 giving a range of structurally diverse SCI) in a forested environment, compared to a rural  
27 background. Furthermore, isoprene emissions exhibit a diurnal cycle in forested environments  
28 owing to a strong temperature dependence, hence are predicted to change significantly in the  
29 future as a response to a changing climate and other environmental conditions (Peñuelas and  
30 Staudt, 2010).

31

## 1 4 Isoprene + Ozone as a function of DMS

### 2 4.1 Results

3 A series of experiments analogous to those reported in Section 3 were performed as a function  
4 of dimethyl sulfide concentration, [DMS], rather than [H<sub>2</sub>O]. Figure 5 shows that SO<sub>2</sub> loss in  
5 the presence of isoprene and ozone is increasingly inhibited by the presence of greater  
6 amounts of DMS. Under the experimental conditions applied, it is assumed that the SCI  
7 produced in isoprene ozonolysis are reacting with DMS in competition with SO<sub>2</sub> (Reaction  
8 R8).

9 Equation E4 is analogous to Equation E3 but for varying [DMS] rather than [H<sub>2</sub>O]. However,  
10 as for the isoprene + O<sub>3</sub> as a function of water experiments described in Section 3, there is  
11 potential for the acid products of the isoprene ozonolysis reaction to provide an additional  
12 sink for SCI in the chamber. Using the same methodology as described in Section 3.2, an  
13 explicit acid term was included in Equation E4 to give Equation E8.

$$14 \quad [\text{SO}_2] \left( \frac{1}{f} - 1 \right) - \frac{k_9}{k_2} [\text{Acid}] = \frac{k_8}{k_2} [\text{DMS}] + \frac{k_3}{k_2} [\text{H}_2\text{O}] + \frac{k_d + L}{k_2} \quad (\text{E8})$$

15 Figure 6 shows a fit of Equation E8 to the experimental data. This yields a gradient of  $k_8/k_2$   
16 and an intercept of  $(k_3[\text{H}_2\text{O}] + k_d + L)/k_2$ . The derived relative rate constant of  
17  $k(\text{SCI}+\text{DMS})/k(\text{SCI}+\text{SO}_2)$ ,  $k_8/k_2$ , using this method is  $3.5 (\pm 1.8)$ . Using the absolute value of  
18  $k_2(\text{CH}_2\text{OO} + \text{SO}_2)$  derived by Welz et al. (as described previously) determines a value of  $k_8 =$   
19  $1.4 (\pm 0.7) \times 10^{-10} \text{ cm}^3 \text{ s}^{-1}$  (Table 2).

20 The intercept of the linear fit in Figure 6, is  $1.0 (\pm 1.7) \times 10^{12} \text{ cm}^{-3}$ . This represents  $(k_3[\text{H}_2\text{O}] +$   
21  $k_d + L)/k_2$  and hence can also be compared with the kinetic parameters derived in Section 3  
22 from the isoprene + O<sub>3</sub> as a function of H<sub>2</sub>O experiments. From Figure 3,  $(k_d + L)/k_2 = 3.0 (\pm$   
23  $3.2) \times 10^{11} \text{ cm}^{-3}$  and  $k_3 [\text{H}_2\text{O}] / k_2 = 2.5 (\pm 0.4) \times 10^{11} \text{ cm}^{-3}$  (with  $[\text{H}_2\text{O}] = 8 \times 10^{15} \text{ cm}^{-3}$ , the  
24 mean of the values for the five DMS experiments ( $6.7 - 8.8 \times 10^{15} \text{ cm}^{-3}$ )), giving a combined  
25 value of  $5.5 (\pm 3.2) \times 10^{11} \text{ cm}^{-3}$ . These two values therefore agree within the precision of the  
26 data.

## 1 4.2 Experimental Uncertainties

2 As noted above, this analysis assumes that the multiple SCI species in reality present in the  
3 ozonolysis system may be analysed as a single species (or exhibit the same reactivity). While  
4 the data indicate that this approximation satisfactorily describes the observed behaviour under  
5 the conditions applied, other work (*e.g.* Taatjes et al., 2013) has shown that reactivity of  
6 different SCIs, and different conformers of the same SCI, can differ, affecting the retrieval of  
7 kinetics in multi-SCI ozonolysis systems; Newland et al. (2015) have illustrated this effect in  
8 the case of *syn*- and *anti*-CH<sub>3</sub>CHOO. Similarly, the response of the SCI population to reaction  
9 with organic acids is approximated by a single reaction with those species observed (*i.e.*  
10 HCOOH, CH<sub>3</sub>COOH). A further assumption made is that the mean isoprene-SCI + SO<sub>2</sub>  
11 reaction rate may be represented by that directly measured for CH<sub>2</sub>OO with SO<sub>2</sub> (Welz et al.,  
12 2012). These approximations introduce systematic uncertainty into the derived rate constants,  
13 but given the lack of fundamental data for individual SCI isomers, it is not possible to  
14 evaluate this. The data obtained are well within the capability of the experimental approaches:  
15 DMS levels were inferred from the known volumetric addition to the chamber and are  
16 thought unlikely to be significantly in error. O<sub>3</sub> and isoprene were monitored using well-  
17 established techniques at levels well above their detection limits. The observed changes in  
18 SO<sub>2</sub> removal upon addition of DMS (as shown in Figure 5) were substantial, well in excess of  
19 the sensitivity limit and uncertainty of the SO<sub>2</sub> monitor. However, it is important to note that  
20 no constraints regarding the products of the proposed DMS + SCI reaction were obtained; OH  
21 reaction with DMS is complex, proceeding through both abstraction and addition/complex  
22 formation channels, the latter rendered partially irreversible under atmospheric conditions  
23 through subsequent reaction with O<sub>2</sub> (Sander et al., 2011). The observed behaviour (Figure 5)  
24 is not consistent with reversible complex formation dominating the SCI-DMS system under  
25 the conditions used; however it is possible that decomposition of such a complex to reform  
26 DMS, or its further reaction (*e.g.* with SO<sub>2</sub>, analogous to the secondary ozonide mechanism  
27 proposed by Hatakeyama et al., 1986) would be consistent with the observed data, and also  
28 imply that the reaction may not lead to net DMS removal. Time-resolved laboratory  
29 measurements and product studies are needed to provide a test of this mechanistic possibility.

### 1 **4.3 Discussion and Atmospheric Implications**

2 To the authors' knowledge, this is the first work to show the relatively fast (in relation to  
3 other recently determined SCI bimolecular reactions, e.g. SCI + SO<sub>2</sub> and NO<sub>2</sub>, and the well  
4 established OH + DMS reaction) rate of reaction of SCI with DMS, although the products  
5 have yet to be identified. While this work presents only SCI derived from isoprene  
6 ozonolysis, it seems likely that the fast reaction rate will apply to all SCI (though the precise  
7 rate will be structure dependent).

8 DMS is mainly produced as a by-product of phytoplankton respiration and so the highest  
9 concentrations are found in marine coastal environments or above active phytoplankton  
10 blooms. Furthermore, Jardine et al. (2015) have recently shown that DMS mixing ratios  
11 within and above a primary Amazonian rainforest ecosystem can reach levels of up to 160  
12 pptv, in canopy and above the surface, for periods of up to 8 hours during the evening and  
13 into the night, with levels peaking at 80 pptv above canopy.

14 SCI can also be expected to be present in the marine environment. As already discussed,  
15 mixing ratios of isoprene (Sinha et al., 2007; Yassaa et al., 2008) and monoterpenes (Yassaa  
16 et al., 2008) have been reported to reach in the region of hundreds of pptv over active  
17 phytoplankton blooms in the marine boundary layer. Additionally, the emission of small  
18 alkenes from coastal waters has been observed (Lewis et al., 1999). Furthermore, the  
19 photolysis of alkyl iodides (prevalent in the coastal environment (Jones et al., 2010)) may be a  
20 significant source of SCI (Stone et al., 2013). Berresheim et al. (2014) have suggested that  
21 small SCI derived from alkyl iodide photolysis may be responsible for observed H<sub>2</sub>SO<sub>4</sub>  
22 production, in excess of that expected from measured SO<sub>2</sub> and OH concentrations, at the  
23 coastal atmospheric observatory Mace Head, Ireland. Jones et al. (2014) proposed SCI  
24 produced from alkyl iodide photolysis as a possible source of surprisingly high formic acid  
25 concentrations observed in the marine environment in the European Arctic. Other non-  
26 ozonolysis sources of SCI include dissociation of the dimethyl sulfoxide (DMSO) peroxy  
27 radical (Asatryan and Bozzelli, 2008; Taatjes et al., 2008) (which could be an important  
28 source in the marine environment, where DMSO is an oxidation product of OH + DMS), and  
29 potentially from reactions of peroxy radicals with OH in remote atmospheres (Fittschen et al.,  
30 2014).

31 From the analysis in Section 3.4 a concentration of ISOP-SCI of  $4.1 \times 10^2$  molecules cm<sup>-3</sup>  
32 was calculated, assuming an isoprene concentration of 1 ppbv. In a remote marine

1 environment isoprene concentrations are probably an order of magnitude lower than this and  
2 consequently [ISOP-SCI] would be calculated to be on the order of  $4 \times 10^1$  molecules  $\text{cm}^{-3}$ .  
3 However, some regions will be impacted by both high isoprene and DMS concentrations, for  
4 example tropical islands, such as Borneo, which can have high isoprene concentrations and  
5 are strongly influenced by marine air masses (MacKenzie et al., 2011), as well as significant  
6 terrestrial sources from vegetation and soils in the Amazon, especially into the evening and at  
7 night (Jardine et al., 2015), when ozonolysis chemistry is at its most effective relative to  
8 photochemical OH chemistry. High sulfate composition of organic aerosols collected from  
9 the Borneo rain forests likely arises from the chemical processing of oceanic emissions of  
10 DMS and  $\text{SO}_2$  (Hamilton et al., 2013). The sulphate content of aerosols was observed to  
11 increase further over oil palm plantations in Borneo, where isoprene concentrations may reach  
12 levels on the order of tens of ppbv (MacKenzie et al., 2011), indicating scope for alkene  
13 ozonolysis – DMS chemical interactions to become significant. If a diurnally averaged [OH]  
14 is taken as  $5 \times 10^5$  molecules  $\text{cm}^{-3}$  then the loss rate of DMS to OH is  $\sim 3.5 \times 10^{-6} \text{ s}^{-1}$  while  
15 the loss to ISOP-SCI, at a concentration of  $1 \times 10^2 \text{ cm}^{-3}$ , is  $\sim 2 \times 10^{-8} \text{ s}^{-1}$ , *i.e.* about 0.4 % of  
16 the loss to OH. However in an environment with particularly high isoprene mixing ratios,  
17 such as over the oil palm plantations in Borneo this could rise to a few percent.

18 SCI derived from isoprene ozonolysis are unlikely to compete with OH during the day-time  
19 or  $\text{NO}_3$  during the night, as an oxidant of DMS. However, alternative SCI sources have been  
20 suggested which may lead to significantly higher SCI concentrations in marine environments  
21 those predicted from ozonolysis alone. Further investigation is required to clarify the reasons  
22 for the observed discrepancies in  $\text{SO}_2$  and DMS oxidation and the possibility that these may  
23 be, at least in part, explained by the presence of SCI, dependent on the products of SCI-DMS  
24 interactions. SCI are most likely of a similar importance to other minor reaction channels for  
25 DMS processing such as reaction with atomic chlorine or BrO, reported to have a reaction  
26 rate constant of  $\sim 3.4 \times 10^{-10} \text{ cm}^3 \text{ molecule}^{-1} \text{ s}^{-1}$  at 298K (Atkinson et al., 2004) and marine  
27 boundary layer concentrations on the order of  $10^3 - 10^4$  molecules  $\text{cm}^{-3}$  (von Glasow and  
28 Crutzen, 2007). SCI may be most important for DMS oxidation during the evening period and  
29 early morning periods, when OH and  $\text{NO}_3$  production are both relatively low.

30

## 1 **5 Conclusions**

2 Isoprene ozonolysis leads to gas-phase SO<sub>2</sub> removal, which decreases significantly with  
3 increasing water vapour. This trend is consistent with production of stabilised Criegee  
4 intermediates (SCIs) from the ozonolysis reaction, and the subsequent reaction of these  
5 species with SO<sub>2</sub> or H<sub>2</sub>O. Competition between H<sub>2</sub>O and SO<sub>2</sub> for reaction with the SCI leads  
6 to this observed relationship, in which SCI abundance is sensitive to water vapour  
7 concentration, even at the dry end of the range found in the troposphere (ca. 1 – 20 % RH).  
8 The kinetics of this system can be described well by treatment of the SCI population as a  
9 single pseudo-SCI species under the experimental conditions applied, allowing for relatively  
10 easy integration into atmospheric chemical models. The results indicate that SCI derived from  
11 isoprene ozonolysis are unlikely to make a substantial contribution to atmospheric SO<sub>2</sub>  
12 oxidation and hence sulphate aerosol formation in the troposphere.

13 Furthermore we show, for the first time, that SO<sub>2</sub> loss in the presence of isoprene and ozone  
14 significantly decreases with the addition of dimethyl sulfide (DMS). The data suggest a fast  
15 reaction of isoprene derived SCI with DMS. However, the exact mechanistic nature of the  
16 reaction, including the likely oxidation products, need to be elucidated. This result has  
17 implications for the oxidation of DMS in the atmosphere. Although it seems unlikely that SCI  
18 produced from isoprene ozonolysis alone are important for DMS oxidation, it is possible that  
19 (the sum of) SCI species produced from other alkene-ozone reactions, or from other  
20 (photo)chemical sources (which may be prevalent in the marine boundary layer), could be a  
21 significant source of DMS oxidant under certain atmospheric conditions, and hence influence  
22 new particle formation above environments influenced by emissions of unsaturated  
23 hydrocarbons and DMS.

24

25

## 26 **Acknowledgements**

27 The assistance of the EUPHORE staff is gratefully acknowledged. Mat Evans, Salim Alam,  
28 Marie Camredon and Stephanie La are thanked for helpful discussions. This work was funded  
29 by EU FP7 EUROCHAMP 2 Transnational Access activity (E2-2012- 05-28-0077), the UK  
30 NERC (NE/K005448/1) and Fundacion CEAM. Fundación CEAM is partly supported by  
31 Generalitat Valenciana, and the project DESESTRES (Prometeo Program - Generalitat

1 Valenciana). EUPHORE instrumentation is partly funded by the Spanish Ministry of Science  
2 and Innovation, through INNPLANTA project: PCT-440000-2010-003. Original data is  
3 available from author on request.  
4



## 1 **References**

- 2 Alam, M. S., Camredon, M., Rickard, A. R., Carr, T., Wyche, K. P., Hornsby, K. E., Monks,  
3 P. S., and Bloss, W. J.: Total radical yields from tropospheric ethene ozonolysis, *Phys. Chem.*  
4 *Chem. Phys.*, 13, 11002–11015, 2011.
- 5 Alam, M. S., Rickard, A. R., Camredon, M., Wyche, K. P., Carr, T., Hornsby, K. E., Monks,  
6 P. S., and Bloss, W. J.: Radical Product Yields from the Ozonolysis of Short Chain  
7 Alkenes under Atmospheric Boundary Layer Conditions, *J. Phys. Chem. A*, 117, 12468-  
8 12483, 2013.
- 9 Anglada, J. M., Gonzalez, J., and Torrent-Sucarrat, M.: Effects of the substituents on the  
10 reactivity of carbonyl oxides. A theoretical study on the reaction of substituted carbonyl  
11 oxides with water, *Phys. Chem. Chem. Phys.*, 13, 13034–13045, 2011.
- 12 Aplincourt, P., and Anglada, J. M.: Theoretical Studies on Isoprene Ozonolysis under  
13 Tropospheric Conditions. 1. Reaction of Substituted Carbonyl Oxides with Water, *J. Phys*  
14 *Chem. A*, 107, 5798-5811, 2003
- 15 Asatryan, R. and Bozzelli, J.W.: Formation of a Criegee intermediate in the low-temperature  
16 oxidation of dimethyl sulfoxide, *Phys. Chem. Chem. Phys.*, 10, 1769–1780, 2008.
- 17 Atkinson, R., Aschmann, S. M., Arey, J., and Shorees, B.: Formation of OH radicals in the  
18 gas-phase reaction of O<sub>3</sub> with a series of terpenes, *J. Geophys. Res.*, 97, 6065–6073, 1992.
- 19 Atkinson, R., Baulch, D. L., Cox, R. A., Crowley, J. N., Hampson, R. F., Hynes, R. G.,  
20 Jenkin, M. E., Rossi, M. J., and Troe, J.: Evaluated kinetic and photochemical data for  
21 atmospheric chemistry: Volume I – gas phase reactions of O<sub>x</sub>, HO<sub>x</sub>, NO<sub>x</sub> and SO<sub>x</sub> species,  
22 *Atmos. Chem. Phys.*, 4, 1461–1738, 2004.
- 23 Atkinson, R., Baulch, D. L., Cox, R. A., Crowley, J. N., Hampson, R. F., Hynes, R. G.,  
24 Jenkin, M. E., Rossi, M. J., Troe, J., and Subcommittee, I.: Evaluated kinetic and  
25 photochemical data for atmospheric chemistry: Volume II – gas phase reactions of organic  
26 species, *Atmos. Chem. Phys.*, 6, 3625–4055, 2006.
- 27 Barnes, I., Hjorth, J., and Mihalopoulos, N.: Dimethylsulfide and dimethylsulfoxide and their  
28 oxidation in the atmosphere, *Chem. Rev.*, 106, 940–975, 2006.
- 29 Becker, K. H.: EUPHORE: Final Report to the European Commission, Contract EV5V-  
30 CT92-0059, Bergische Universität Wuppertal, Germany, 1996.

1 Berndt, T., Voigtländer, J., Stratmann, F., Junninen, H., Mauldin III, R. L., Sipilä, M.,  
2 Kulmala, M., and Herrmann, H.: Competing atmospheric reactions of CH<sub>2</sub>OO with SO<sub>2</sub> and  
3 water vapour, *Phys. Chem. Chem. Phys.*, 16, 19130–19136, 2014.

4 Berresheim, H., Adam, M., Monahan, C., O'Dowd, C., Plane, J. M. C., Bohn, B., and Rohrer  
5 F.: Missing SO<sub>2</sub> oxidant in the coastal atmosphere? – observations from high-resolution  
6 measurements of OH and atmospheric sulfur compounds, *Atmos. Chem. Phys.*, 14, 12209-  
7 12223, 2014.

8 Calvert, J. G., Atkinson, R., Kerr, J. A., Madronich, S., Moortgat, G. K., Wallington, T. J.,  
9 and Yarwood, G.: *The Mechanism of Atmospheric Oxidation of the Alkenes*, Oxford  
10 University Press, New York, USA, 552 pp., 2000.

11 Chao, W., Hsieh, J. -T., Chang C. -H., and Lin J. J. -M.: Direct kinetic measurement of the  
12 reaction of the simplest Criegee intermediate with water vapour, *Science*, DOI:  
13 10.1126/science.1261549, 2015.

14 Charlson, R. J., Lovelock, J. E., Andreae, M. O., and Warren, S. G.: Oceanic phytoplankton,  
15 atmospheric sulphur, cloud albedo and climate, *Nature*, 326, 655–661, 1987.

16 Chhantyal-Pun, R., Davey, A., Shallcross, D. E., Percival, C. J., and Orr-Ewing, A. J.: A  
17 kinetic study of the CH<sub>2</sub>OO Criegee intermediate self-reaction, reaction with SO<sub>2</sub> and  
18 unimolecular reaction using cavity ring-down spectroscopy, *Phys. Chem. Chem. Phys.*, 17,  
19 3617-3626, 2015.

20 Cox, R. A., and Penkett, S. A.: Oxidation of atmospheric SO<sub>2</sub> by products of the ozone-olefin  
21 reaction, *Nature*, 230, 321-322, 1971.

22 Curci, R., Dinoi, A., and Rubino, M. F.: Dioxirane oxidations: Taming the reactivity-  
23 selectivity principle, *Pure & Appl. Chem.*, 67, 811-822, 1995.

24 Curtis, A. R., and Sweetenham, W. P.: *Facsimile/Checkmat User's Manual*, Harwell  
25 Laboratory, Oxfordshire, 1987.

26 Faloon, I.: Sulfur processing in the marine atmospheric boundary layer: A review and  
27 critical assessment of modeling uncertainties, *Atmos. Environ.*, 43, 2841-2854, 2009.

28 Fenske, J. D., Hasson, A. S., Ho, A. W., and Paulson, S. E.: Measurement of absolute  
29 unimolecular and bimolecular rate constants for CH<sub>3</sub>CHOO generated by the trans-2-butene  
30 reaction with ozone in the gas phase, *J. Phys. Chem. A*, 104, 9921–9932, 2000.

1 Fittschen, C., Whalley, L. K., and Heard, D. E.: The reaction of  $\text{CH}_3\text{O}_2$  radicals with OH  
2 radicals: a neglected sink for  $\text{CH}_3\text{O}_2$  in the remote atmosphere, *Environ. Sci. Technol.*, 48,  
3 7700–7701, 2014.

4 Gravestock, T. J., Blitz, M. A., Bloss, W. J., and Heard, D. E.: A multidimensional study of  
5 the reaction  $\text{CH}_2\text{I}+\text{O}_2$ : Products and atmospheric implications, *ChemPhysChem*, 11, 3928 –  
6 3941, 2010.

7 Guenther, A., Hewitt, C. N., Erickson, D., Fall, R., Geron, C., Graedel, T., Harley, P.,  
8 Klinger, L., Lerdau, M., McKay, W. A., Scholes, B., Steinbrecher, R., Tallamraju, R., Taylor,  
9 J., and Zimmerman, P.: A global model of natural volatile organic compound emissions, *J.*  
10 *Geophys. Res.*, 100, 8873–8892, 1995.

11 Hamilton, J. F., Alfarra, M. R., Robinson, N., Ward, M. W., Lewis, A. C., McFiggans, G. B.,  
12 Coe, H., and Allan, J. D.: Linking biogenic hydrocarbons to biogenic aerosol in the Borneo  
13 rainforest, *Atmos. Chem. Phys.*, 13, 11295–11305, 2013.

14 Hasson, A. S., Orzechowska, G., and Paulson, S. E.: Production of stabilized Criegee  
15 intermediates and peroxides in the gas phase ozonolysis of alkenes 1. Ethene, trans-2-butene,  
16 and 2,3-dimethyl-2-butene, *J. Geophys. Res.*, 106, 34131–34142, 2001.

17 Hatakeyama, S., Kobayashi, H., Lin, Z.-Y., Takagi, H., and Akimoto, H.: Mechanism for the  
18 reaction of  $\text{CH}_2\text{OO}$  with  $\text{SO}_2$ , *J. Phys. Chem.*, 90, 4131–4135, 1986.

19 Jardine, K., Yañez-Serrano, A. M., Williams, J., Kunert, N., Jardine, A., Taylor, T., Abrell,  
20 L., Artaxo, P., Guenther, A., Hewitt, C. N., House, E., Florentino, A. P., Manzi, A, Higuchi,  
21 N., Kesselmeier, J., Behrendt, T., Veres, P. R., Derstroff, B., Fuentes, J. D., Martin, S. T., and  
22 Andreae, M. O.: Dimethyl sulfide in the Amazon rain forest, *Global Biogeochem. Cycles*, 29,  
23 doi:10.1002/2014GB004969, 2015.

24 Jenkin, M. E., Saunders, S. M., and Pilling, M. J.: The tropospheric degradation of volatile  
25 organic compounds: a protocol for mechanism development, *Atmos. Environ.*, 31, 81–104,  
26 1997.

27 Johnson, D. and Marston, G.: The gas-phase ozonolysis of unsaturated volatile organic  
28 compounds in the troposphere, *Chem. Soc. Rev.*, 37, 699–716, 2008.

29 Jones, B. T., Muller, J. B. A., O’Shea, S. J., Bacak, A., Le Breton, M., Bannan, T. J., Leather,  
30 K. E., Booth, A. M., Illingworth, S., Bower, K., Gallagher, M. W., Allen, G., Shallcross, D.

1 E., Bauguitte, S. J. -B., Pyle, J. A., and Percival C. J.: Airborne measurements of HC(O)OH  
2 in the European Arctic: A winter – summer comparison, *Atmos. Environ.*, 99, 556-567,  
3 2014.

4 Jones, C. E., Hornsby, K. E., Sommariva, R., Dunk, R. M., von Glasow, R., McFiggans, G.,  
5 and Carpenter, L. J.: Quantifying the contribution of marine organic gases to atmospheric  
6 iodine, *Geophys. Res. Lett.*, 37, L18804, doi:10.1029/2010GL043990, 2010.

7 Kjaergaard, H. G., Kurtén, T., Nielsen, L. B., Jørgensen, S., and Wennberg, P. O.: Criegee  
8 Intermediates React with Ozone, *J. Phys. Chem. Lett.*, 4, 2525-2529, 2013.

9 Kuwata, K. T., Hermes, M. R., Carlson, M. J., and Zogg, C. K.: Computational Studies of  
10 the Isomerization and Hydration Reactions of Acetaldehyde Oxide and Methyl Vinyl  
11 Carbonyl Oxide, *J. Phys Chem. A*, 114, 9192-9204, 2010.

12 Kuwata, K. T., Valin, L. C., and Converse, A. D.: Quantum Chemical and Master Equation  
13 Studies of the Methyl Vinyl Carbonyl Oxides Formed in Isoprene Ozonolysis, *J. Phys.*  
14 *Chem. A*, 109, 10710-10725, 2005.

15 Lewis, A. C., McQuaid, J. B., Carslaw, N., and Pilling, M. J.: Diurnal cycles of short-lived  
16 tropospheric alkenes at a north Atlantic coastal site, *Atmos. Environ.*, 33, 2417–2422, 1999.

17 Lewis, T. R., Blitz, M. A., Heard, D. E., and Seakins, P. W.: Direct evidence for a substantive  
18 reaction between the Criegee intermediate, CH<sub>2</sub>OO, and the water vapour dimer, *Phys. Chem.*  
19 *Chem. Phys.*, 17, 4859-4863, 2015.

20 MacKenzie, A. R., Langford, B., Pugh, T. A. M., Robinson, N., Misztal, P. K., Heard, D. E.,  
21 Lee, J. D., Lewis, A. C., Jones, C. E., Hopkins, J. R., Philips, G., Monks, P. S., Karunaharan,  
22 A., Hornsby, K. E., Nicolas-Perea, V., Coe, H., Whalley, L. K., Edwards, P. M., Evans, M. J.,  
23 Stone, D., Ingham, T., Commane, R., Furneaux, K. L., McQuaid, J., Nemitz, E., Seng, Y. K.,  
24 Fowler, D., Pyle, J. A., and Hewitt, C. N.: The atmospheric chemistry of trace gases and  
25 particulate matter emitted by different land uses in Borneo, *Phil. Trans. R. Soc. B*, 366, 3177–  
26 3195, 2011.

27 Malkin, T. L., Goddard, A., Heard, D. E., and Seakins, P. W.: Measurements of OH and HO<sub>2</sub>  
28 yields from the gas phase ozonolysis of isoprene, *Atmos. Chem. Phys.*, 10, 1441-1459, 2010.

29 Martinez, R. I., and Herron, J. T.: Stopped-flow studies of the mechanisms of alkene-ozone  
30 reactions in the gas-phase: tetramethylethylene, *J. Phys. Chem.*, 91, 946-953, 1987.

1 Mauldin III, R. L., Berndt, T., Sipilä, M., Paasonen, P., Petäjä, T., Kim, S., Kurtén, T.,  
2 Stratmann, F., Kerminen, V.-M., and Kulmala, M.: A new atmospherically relevant oxidant,  
3 Nature, 488, 193–196, 2012.

4 Moore, R. M., Oram, D. E., and Penkett, S. A.: Production of isoprene by marine  
5 phytoplankton cultures, Geophys. Res. Lett., 21, 2507-2510, 1994.

6 Neeb, P., Sauer, F., Horie, O., and Moortgat, G. K.: Formation of hydroxymethyl  
7 hydroperoxide and formic acid in alkene ozonolysis in the presence of water vapour, Atmos.  
8 Environ., 31, 1417–1423, 1997.

9 Newland, M. J., Rickard, A. R., Alam, M. S., Vereecken, L., Muñoz, A., Ródenas, M., and  
10 Bloss, W. J.: Kinetics of stabilised Criegee intermediates derived from alkene ozonolysis:  
11 reactions with SO<sub>2</sub>, H<sub>2</sub>O and decomposition under boundary layer conditions, Phys. Chem.  
12 Chem. Phys., 17, 4076, 2015.

13 Niki, H., Maker, P. D., Savage, C. M., Breitenbach, L. P., and Hurley, M. D.: FTIR  
14 spectroscopic study of the mechanism for the gas-phase reaction between ozone and  
15 tetramethylethylene, J. Phys. Chem, 91, 941-946, 1987.

16 Novelli, A., Vereecken, L., Lelieveld, J., and Harder, H.: Direct observation of OH formation  
17 from stabilised Criegee intermediates, Phys. Chem. Chem. Phys., 16, 19941-19951, 2014.

18 Noziere, B., Kalberer, M., Claeys, M., Allan, J., D’Anna, B., Decesari, S., Finessi,  
19 E., Glasius, M., Grgić, I., Hamilton, J. F., Hoffmann, T., Iinuma, Y., Jaoui, M., Kahnt,  
20 A., Kampf, C. J., Kourtchev, I., Maenhaut, W., Marsden, N., Saarikoski, S., Schnelle-Kreis,  
21 J., Surratt, J. D., Szidat, S., Szmigielski, R., and Wisthaler, A.: The Molecular Identification  
22 of Organic Compounds in the Atmosphere: State of the Art and Challenges, Chem. Rev.,  
23 doi: 10.1021/cr5003485, 2015.

24 Olzmann, M., Kraka, E., Cremer, D., Gutbrod, R., and Andersson, S.: Energetics, Kinetics,  
25 and Product Distributions of the Reactions of Ozone with Ethene and 2,3-Dimethyl-2-  
26 butene, J. Phys. Chem. A, 101, 9421-9429, 1997.

27 Ouyang, B., McLeod, M. W., Jones, R. L., and Bloss, W. J.: NO<sub>3</sub> radical production from the  
28 reaction between the Criegee intermediate CH<sub>2</sub>OO and NO<sub>2</sub>, Phys. Chem. Chem. Phys., 15,  
29 17070-17075, 2013.

1 Paulson, S. E., Chung, M., Sen, A. D., and Orzechowska, G.: Measurement of OH radical  
2 formation from the reaction of ozone with several biogenic alkenes, *Geophys. Res. Lett.*, 24,  
3 3193–3196, 1997.

4 Peñuelas, J., and Staudt, M.: BVOCs and global change, *Trends Plant Sci.*, 15, 133-144, 2010.

5 Prousek, J.: Chemistry of Criegee Intermediates, *Chem. Listy*, 103, 271-276, 2009.

6 Read, K. A., Lewis, A. C., Bauguitte, S., Rankin, A. M., Salmon, R. A., Wolff, E. W., Saiz-  
7 Lopez, A., Bloss, W. J., Heard, D. E., Lee, J. D., and Plane, J. M. C.: DMS and MSA  
8 measurements in the Antarctic Boundary Layer: impact of BrO on MSA production, *Atmos.*  
9 *Chem. Phys.*, 8, 2985–2997, 2008.

10 Rickard, A. R., Johnson, D., McGill, C. D., and Marston, G.: OH Yields in the Gas-Phase  
11 reactions of Ozone with Alkenes, *J. Phys. Chem. A*, 103, 7656–7664, 1999.

12 Sander, S. P., Abbatt, J., Barker, J. R., Burkholder, J. B., Friedl, R. R., Golden, D. M., Huie,  
13 R. E., Kolb, C. E., Kurylo, M. J., Moortgat, G. K., Orkin, V. L., and Wine, P. H.: Chemical  
14 Kinetics and Photochemical Data for Use in Atmospheric Studies, Evaluation No. 17, JPL  
15 Publication 10-6, Jet Propulsion Laboratory, Pasadena, 2011

16 Saunders, S. M., Jenkin, M. E., Derwent, R. G., and Pilling, M. J.: Protocol for the  
17 development of the Master Chemical Mechanism, MCM v3 (Part A): Tropospheric  
18 degradation of non-aromatic volatile organic compounds, *Atmos. Chem. Phys.*, 3, 161-180,  
19 2003.

20 Sheps, L.: Absolute Ultraviolet Absorption Spectrum of a Criegee Intermediate  $\text{CH}_2\text{OO}$ , *J.*  
21 *Phys. Chem. Letts.*, 4, 4201-4205, 2013.

22 Sheps, L., Scully, A. M., and Au, K.: UV absorption probing of the conformer-dependent  
23 reactivity of a Criegee intermediate  $\text{CH}_3\text{CHOO}$  *Phys. Chem. Chem. Phys.*, 16, 26701-26706,  
24 2014.

25 Sindelarova, K., Granier, C., Bouarar, I., Guenther, A., Tilmes, S., Stavrou, T., Müller, J.-  
26 F., Kuhn, U., Stefani, P., and Knorr, W.: Global data set of biogenic VOC emissions  
27 calculated by the MEGAN model over the last 30 years, *Atmos. Chem. Phys.*, 14, 9317-934,  
28 2014.

29 Sinha, V., Williams, J., Meyerhöfer, M., Riebesell, U., Paulino, A. I., and Larsen, A.: Air-sea  
30 fluxes of methanol, acetone, acetaldehyde, isoprene and DMS from a Norwegian fjord

1 following a phytoplankton bloom in a mesocosm experiment, *Atmos. Chem. Phys.*, 7, 739-  
2 755, 2007.

3 Sipilä, M., Jokinen, T., Berndt, T., Richters, S., Makkonen, R., Donahue, N. M.,  
4 Mauldin III, R. L., Kurtén, T., Paasonen, P., Sarnela, N., Ehn, M., Junninen, H.,  
5 Rissanen, M. P., Thornton, J., Stratmann, F., Herrmann, H., Worsnop, D. R., Kulmala, M.,  
6 Kerminen, V.-M., and Petäjä, T.: Reactivity of stabilized Criegee intermediates (sCIs) from  
7 isoprene and monoterpene ozonolysis toward SO<sub>2</sub> and organic acids, *Atmos. Chem. Phys.*, 14,  
8 12143-12153, 2014.

9 Stark, H., Brown, S. S., Goldan, P. D., Aldener, M., Kuster, W. C., Jakoubek, R., Fehsenfeld,  
10 F. C., Meagher, J., Bates, T. S., and Ravishankara, A. R.: Influence of nitrate radical on the  
11 oxidation of dimethyl sulfide in a polluted marine environment, *J. Geophys. Res.*, 112,  
12 D10S10, doi:10.1029/2006JD007669, 2007.

13 Stone, D., Blitz, M., Daubney, L., Howes, N. U. M., and Seakins, P.: Kinetics of CH<sub>2</sub>OO  
14 reactions with SO<sub>2</sub>, NO<sub>2</sub>, NO, H<sub>2</sub>O, and CH<sub>3</sub>CHO as a function of pressure, *Phys. Chem.*  
15 *Chem. Phys.*, 16, 1139-1149, 2014.

16 Stone, D., Blitz, M., Daubney, L., Ingham, T., and Seakins, P.: CH<sub>2</sub>OO Criegee biradical  
17 yields following photolysis of CH<sub>2</sub>I<sub>2</sub> in O<sub>2</sub>, *Phys. Chem. Chem. Phys.*, 15, 19119–19124,  
18 2013.

19 Su, Y. -T., Lin, H. -Y., Putikam, R., Matsui, H., Lin, M. C., and Lee, Y. -P.: Extremely rapid  
20 self-reaction of the simplest Criegee intermediate CH<sub>2</sub>OO and its implications in atmospheric  
21 chemistry, *Nature Chemistry*, 6, 477-483, 2014.

22 Taatjes, C. A., Meloni, G., Selby, T. M., Trevitt, A. J., Osborn, D. L., Percival, C. J., and  
23 Shallcross, D. E.: Direct observation of the Gas-Phase Criegee Intermediate (CH<sub>2</sub>OO), *J. Am.*  
24 *Chem. Soc.*, 130, 11883-11885, 2008

25 Taatjes, C. A., Welz, O., Eskola, A. J., Savee, J. D., Osborn, D. L., Lee, E. P. F., Dyke, J. M.,  
26 Mok, D. W. K., Shallcross, D. E., and Percival, C. J.: Direct measurements of Criegee  
27 intermediate (CH<sub>2</sub>OO) formed by reaction of CH<sub>2</sub>I with O<sub>2</sub>, *Phys. Chem. Chem. Phys.*, 14,  
28 10391-10400, 2012.

29 Taatjes, C. A., Welz, O., Eskola, A. J., Savee, J. D., Scheer, A. M., Shallcross, D. E.,  
30 Rotavera, B., Lee, E. P. F., Dyke, J. M., Mok, D. K. W., Osborn, D. L., and Percival, C. J.:

1 Direct Measurements of Conformer-Dependent Reactivity of the Criegee Intermediate  
2  $\text{CH}_3\text{CHOO}$ , *Science*, 340, 177–180, 2013.

3 Vereecken, L., Harder, H., and Novelli, A.: The reaction of Criegee intermediates with  $\text{NO}$ ,  
4  $\text{RO}_2$ , and  $\text{SO}_2$ , and their fate in the atmosphere, *Phys. Chem. Chem. Phys.*, 14, 14682–14695,  
5 2012.

6 Vereecken, L., Harder, H., and Novelli, A.: The reactions of Criegee intermediates with  
7 alkenes, ozone and carbonyl oxides, *Phys. Chem. Chem. Phys.*, 16, 4039-4049, 2014

8 von Glasow, R., and Crutzen, P. J.: Tropospheric Halogen Chemistry, H. D. Holland and K.  
9 K. Turekian (eds), *Treatise on Geochemistry Update 1*, vol. 4.02, 1-67, 2007.

10 Wei, W., Zheng, R., Pan, Y., Wu, Y., Yang, F., and Hong, S.: Ozone Dissociation to  
11 Oxygen Affected by Criegee Intermediate, *J. Phys. Chem. A*, 118, 1644-1650, 2014.

12 Welz, O., Eskola, A. J., Sheps, L., Rotavera, B., Savee, J. D., Scheer, A. M., Osborn, D. L.,  
13 Lowe, D., Murray Booth, A., Xiao, P., Anwar H., Khan, M., Percival, C. J., Shallcross, D. E.,  
14 and Taatjes, C. A.: Rate coefficients of C1 and C2 Criegee intermediate reactions with formic  
15 and acetic acid near the collision limit: direct kinetics measurements and atmospheric  
16 implications, *Angew. Chem. Int. Ed. Engl.*, 53, 4547–4550, 2014.

17 Welz, O., Savee, J. D., Osborn, D. L., Vasu, S. S., Percival, C. J., Shallcross, D. E., and  
18 Taatjes, C. A.: Direct Kinetic Measurements of Criegee Intermediate ( $\text{CH}_2\text{OO}$ ) Formed by  
19 Reaction of  $\text{CH}_2\text{I}$  with  $\text{O}_2$ , *Science*, 335, 204–207, 2012.

20 Williams, J., Custer, T., Riede, H., Sander, R., Jöckel, P., Hoor, P., Pozzer, A., Wong-  
21 Zehnpfennig, S., Hosaynali Beygi, Z., Fischer, H., Gros, V., Colomb, A., Bonsang, B.,  
22 Yassaa, N., Peeken, I., Atlas, E. L., Waluda, C. M., Van Ardenne, J. A., and Lelieveld, J.:  
23 Assessing the effect of marine isoprene and ship emissions on ozone, using modelling and  
24 measurements from the South Atlantic Ocean, *Environ. Chem.*, 7, 171-182, 2010.

25 Wingenter, O. W., Sive, B. C., Blake, N. J., Blake, D. R., and Rowland, F. S.: Atomic  
26 chlorine concentrations derived from ethane and hydroxyl measurements over the  
27 equatorial Pacific Ocean: Implication for dimethyl sulfide and bromine monoxide, *J.*  
28 *Geophys. Res.*, 110, D20308, doi:10.1029/2005JD005875, 2005.

29 Yassaa, N., Peeken, I., Zöllner, E., Bluhm, K., Arnold, S., Spracklen, D., and Williams, J.:  
30 Evidence for marine production of monoterpenes, *Environ. Chem.*, 5, 391-401, 2008.



- 1 Zhang, D., Lei, W., and Zhang, R.: Mechanism of OH formation from ozonolysis of isoprene:
- 2 kinetics and product yield, *Chem. Phys. Lett.*, 358, 171–179, 2002.
- 3

1 Table 1. Total isoprene SCI yields derived in this work and reported in the literature.

$\Phi_{\text{ISOP-SCI}}$	Reference	Methodology
0.56 ( $\pm 0.03$ )	This work	SO <sub>2</sub> loss
0.58 ( $\pm 0.26$ )	Sipilä <i>et al.</i> (2014)	Formation of H <sub>2</sub> SO <sub>4</sub>
0.30 ( $\Phi_{\text{CH}_2\text{OO}}$ ) <sup>a</sup>	Neeb <i>et al.</i> (1997)	HMHP <sup>b</sup> yield
0.26	Hasson <i>et al.</i> (2001)	Sum of difference between HMHP and H <sub>2</sub> O <sub>2</sub> yields at high / low [H <sub>2</sub> O]
0.28	Rickard <i>et al.</i> (1999)	Assumes stabilisation of 40% of CH <sub>2</sub> OO produced + difference between MVK and MACR production at high / low [SO <sub>2</sub> ]
0.53	Rickard <i>et al.</i> (1999)	Assuming 95% of CH <sub>2</sub> OO is stabilised (after Zhang <i>et al.</i> <sup>23</sup> ) + difference between MVK and MACR production at high / low [SO <sub>2</sub> ]
0.57	Zhang <i>et al.</i> (2002)	Theoretical
0.22	MCMv3.2 <sup>c</sup>	Based on a weighted average of the yields for propene, 1-octene and 2-methyl propene.

2 Uncertainty ranges ( $\pm 2\sigma$ , parentheses) indicate combined precision and systematic measurement error  
 3 components for this work, and are given as stated for literature studies. All referenced experimental studies  
 4 produced SCI from C<sub>5</sub>H<sub>8</sub> + O<sub>3</sub> and were conducted between 700 and 760 Torr. <sup>a</sup> Yield of stabilised CH<sub>2</sub>OO only,  
 5 <sup>b</sup> Hydroxymethyl hydroperoxide (a first order product of CH<sub>2</sub>OO + H<sub>2</sub>O). <sup>c</sup> <http://mcm.leeds.ac.uk/MCM/>  
 6 (Jenkin *et al.*, 1997).

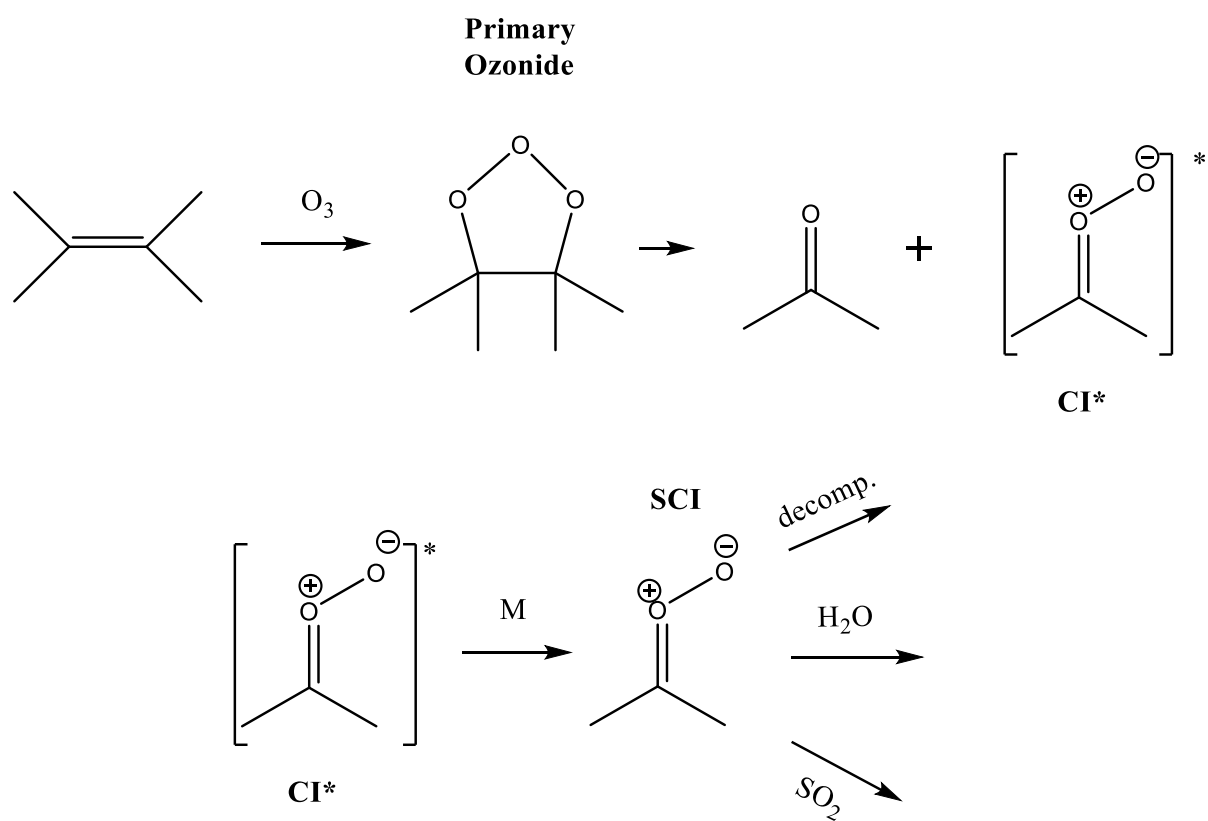
7  
 8  
 9  
 10  
 11  
 12  
 13  
 14  
 15

1 Table 2. Isoprene derived SCI relative and absolute rate constants derived in this work <sup>a</sup>

SCI	$10^5 k_3/k_2$	$10^{15} k_3$ ( $\text{cm}^3 \text{s}^{-1}$ )	$10^{-11} k_d/k_2$ ( $\text{cm}^{-3}$ )	$k_d$ ( $\text{s}^{-1}$ )	$k_8/k_2$	$10^{10} k_8$ ( $\text{cm}^3 \text{s}^{-1}$ )
CH <sub>2</sub> OO <sup>b</sup>	3.3 ( $\pm 1.1$ )	1.3 ( $\pm 0.4$ )	-2.3 <sup>c</sup> ( $\pm 3.5$ )	-8.8 <sup>c</sup> ( $\pm 13$ )		
ISOP-SCI	3.1 ( $\pm 0.5$ )	1.2 ( $\pm 0.2$ )	3.0 ( $\pm 3.2$ )	12 ( $\pm 12$ )	3.5 ( $\pm 2.2$ )	1.4 ( $\pm 0.7$ )
CRB-SCI	2.9 ( $\pm 0.7$ )	1.1 ( $\pm 2.7$ )	6.6 ( $\pm 7.0$ )	26 ( $\pm 27$ )		

2 Uncertainty ranges ( $\pm 2\sigma$ , parentheses) indicate combined precision and systematic measurement error  
 3 components. <sup>a</sup> Scaled to an absolute value using  $k_2(\text{CH}_2\text{OO}) = 3.9 \times 10^{-11} \text{ cm}^3 \text{ s}^{-1}$  (Welz et al., 2012). <sup>b</sup> From  
 4 Newland *et al.* (2015). <sup>c</sup> Values are indistinguishable from zero within the measurement uncertainties.

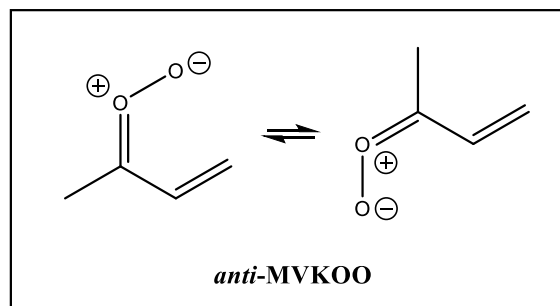
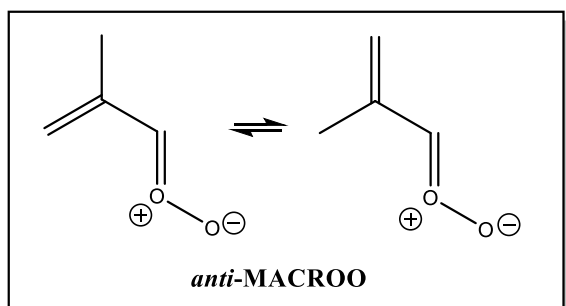
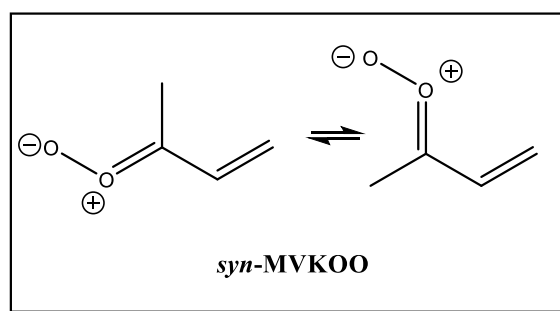
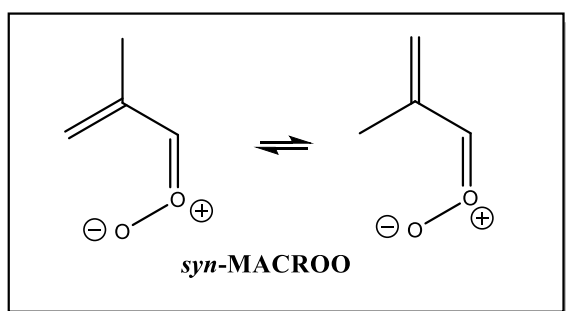
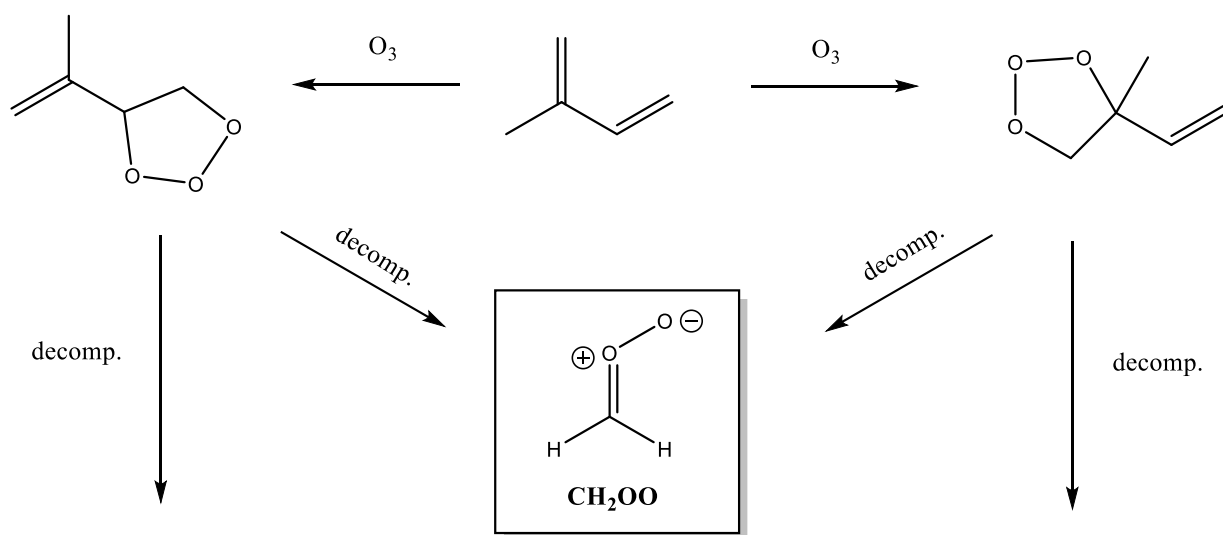
5  
6  
7  
8  
9  
10  
11  
12  
13  
14  
15  
16  
17  
18



1  
2

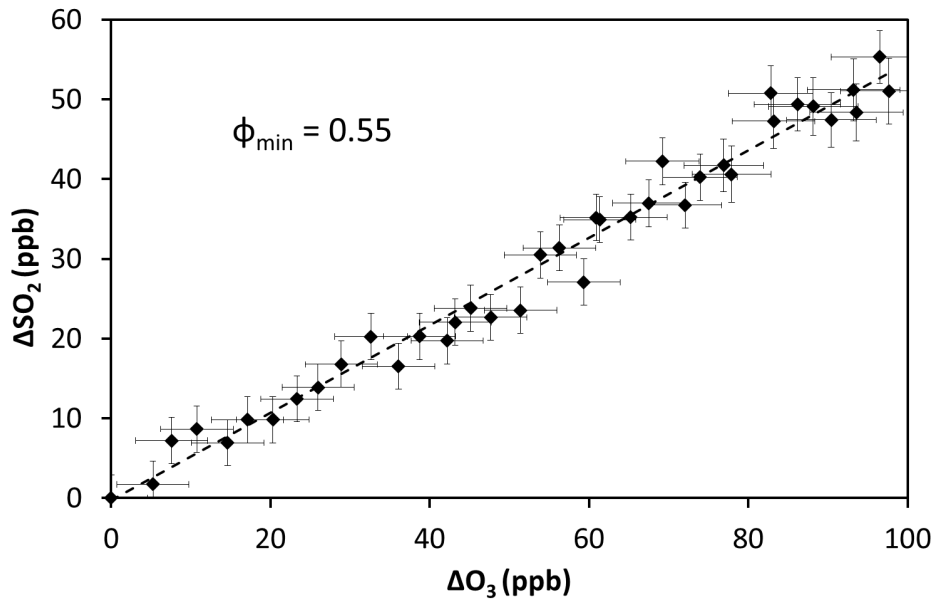
3 Scheme 1. Simplified generic mechanism for the reaction of Criegee Intermediates (CIs)  
4 formed from alkene ozonolysis.

5  
6  
7  
8  
9  
10  
11  
12  
13  
14  
15



1  
2 Scheme 2. Mechanism of formation of the nine possible Criegee Intermediates (CIs) from  
3 isoprene ozonolysis.

4  
5  
6  
7  
8  
9



1

2 Figure 1.  $\Delta SO_2$  .vs.  $\Delta O_3$  during the excess  $SO_2$  experiments ( $[H_2O] < 5 \times 10^{15} \text{ cm}^{-3}$ ). The  
 3 gradient determines the minimum SCI yield ( $\phi_{\min}$ ) from isoprene ozonolysis.

4

5

6

7

8

9

10

11

12

13

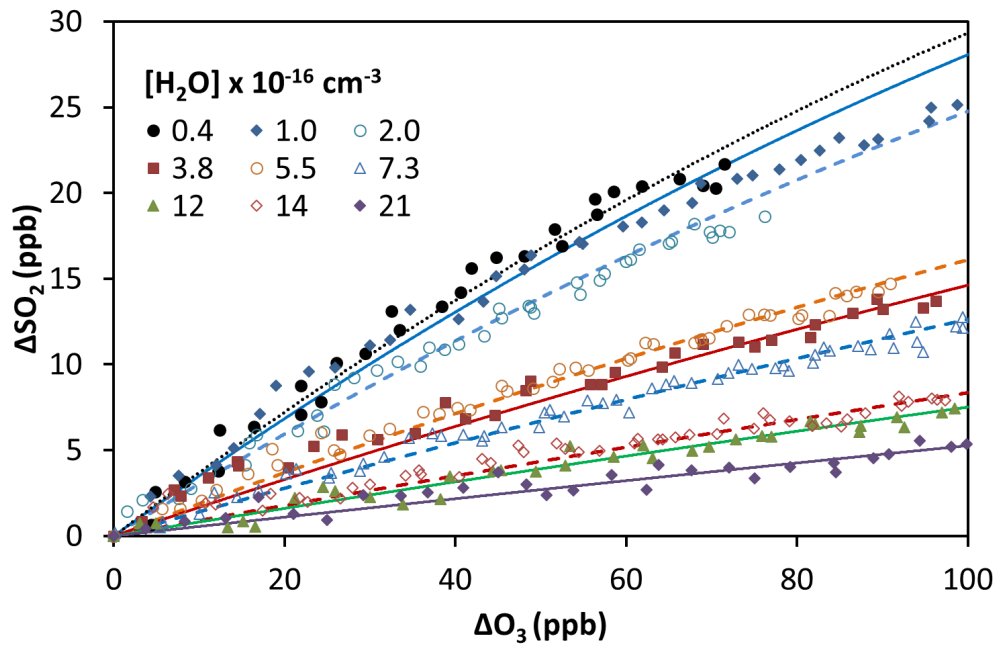
14

15

16

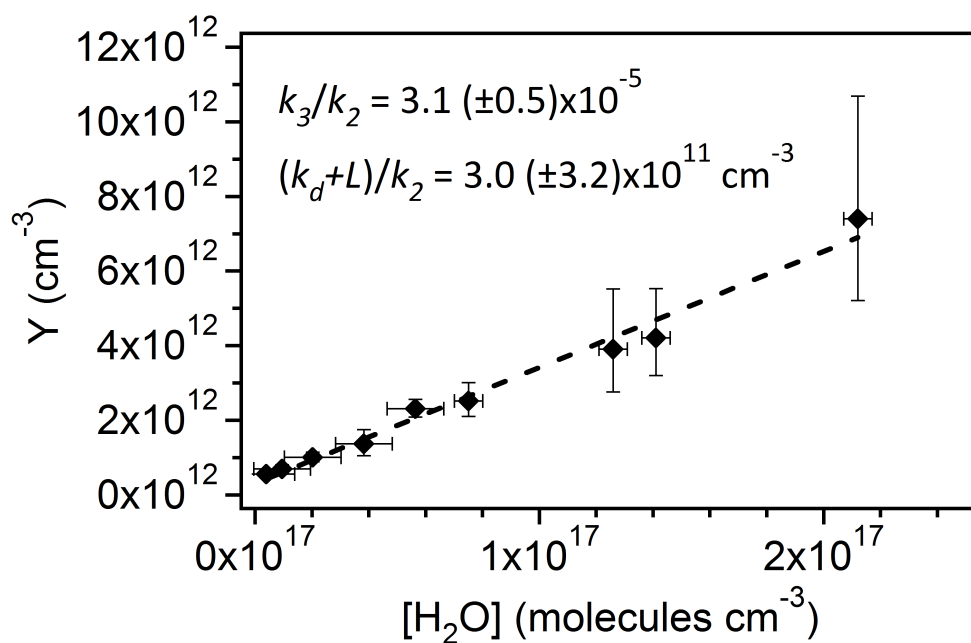
17

18



1  
 2 Figure 2. Cumulative consumption of SO<sub>2</sub> and O<sub>3</sub>, ΔSO<sub>2</sub> versus ΔO<sub>3</sub>, for the ozonolysis of  
 3 isoprene in the presence of SO<sub>2</sub> at a range of water vapour concentrations, from  $4 \times 10^{15} \text{ cm}^{-3}$   
 4 to  $2.1 \times 10^{17} \text{ cm}^{-3}$ . Symbols are experimental data corrected for chamber dilution. Lines are  
 5 smoothed fits to the experimental data.

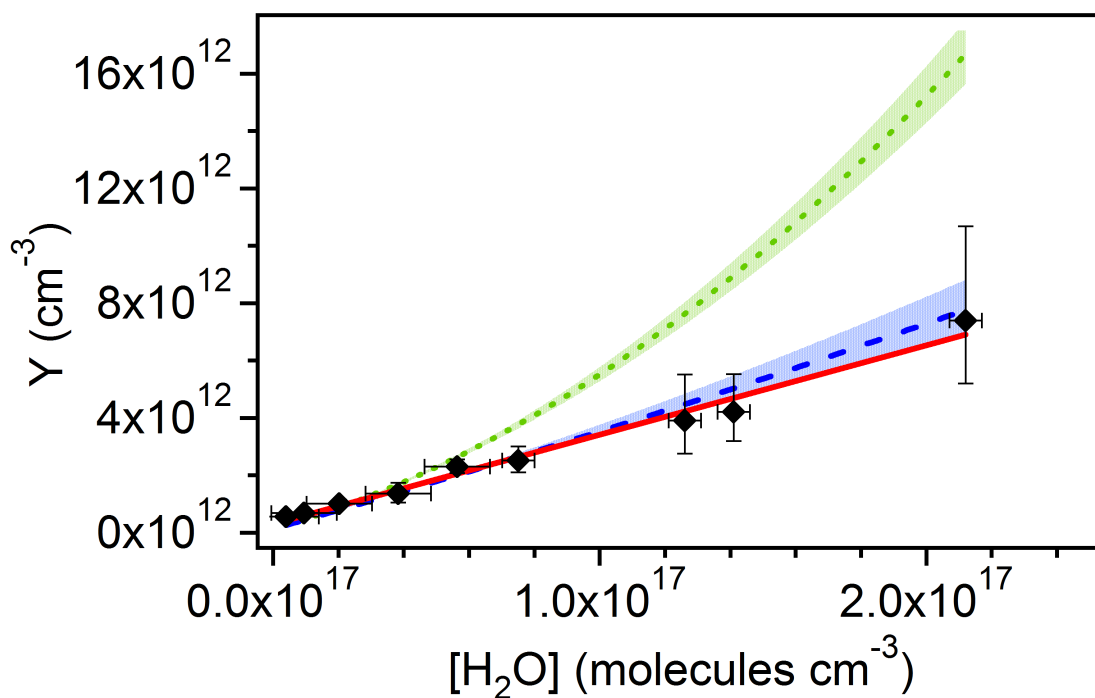
6  
 7  
 8  
 9  
 10  
 11  
 12  
 13  
 14  
 15  
 16  
 17  
 18



1  
 2 Figure 3. Application of Equation E5 to derive relative rate constants for reaction of the  
 3 isoprene derived SCI with H<sub>2</sub>O ( $k_3/k_2$ ) and decomposition ( $(k_d+L)/k_2$ ).  $Y = [\text{SO}_2]((1/f)-1) -$   
 4  $k_9[\text{acid}]/k_2$ .

5  
 6  
 7  
 8  
 9  
 10  
 11  
 12  
 13  
 14  
 15  
 16  
 17  
 18

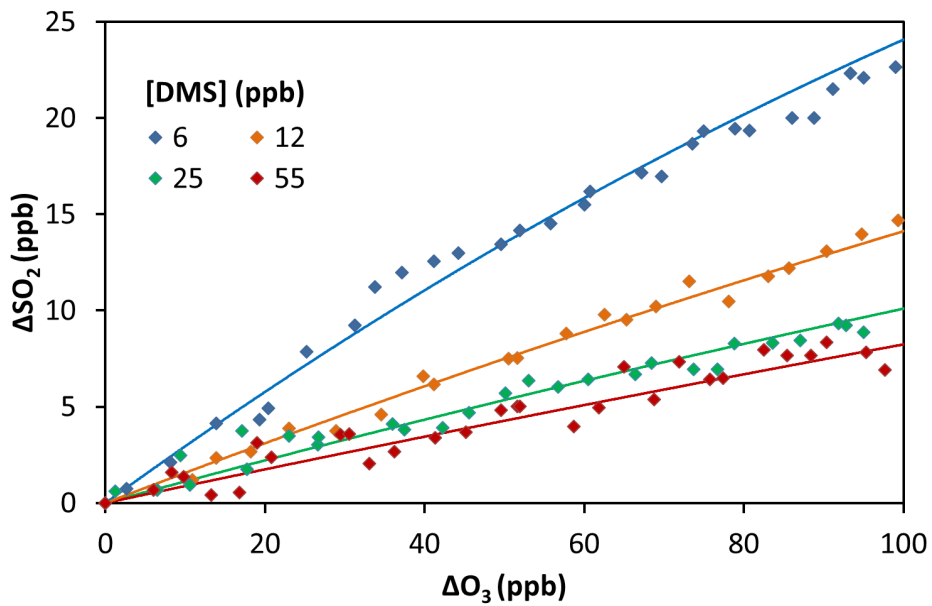




1  
 2 Figure 4. Application of Equation E5 to derive relative rate constants for reaction of the sum  
 3 of the MVKOO and MACROO SCI (CRB-SCI) with the water monomer, and the  
 4 decomposition rate. Red line: water monomer only reactions; blue dashed line: water  
 5 monomer reaction and CH<sub>2</sub>OO water dimer reaction rate from Newland et al. (2015); green  
 6 dotted line: CH<sub>2</sub>OO water dimer reaction rate from Chao et al. (2015). Shaded areas indicate  
 7 reported uncertainties on dimer reaction rates.  $Y = [\text{SO}_2]((1/f)-1) - k_9[\text{acid}]/k_2$ .

8  
 9  
 10  
 11  
 12  
 13  
 14  
 15  
 16  
 17

1



2

3 Figure 5. Cumulative consumption of  $SO_2$  and  $O_3$ ,  $\Delta SO_2$  versus  $\Delta O_3$ , for the ozonolysis of  
4 isoprene in the presence of  $SO_2$  at a range of DMS concentrations, from 6 ppbv to 55 ppbv.  
5  $[H_2O]$  in all experiments was  $< 9 \times 10^{15} \text{ cm}^{-3}$ . Markers are experimental data, corrected for  
6 chamber dilution. Solid lines are smoothed fits to the experimental data.

7

8

9

10

11

12

13

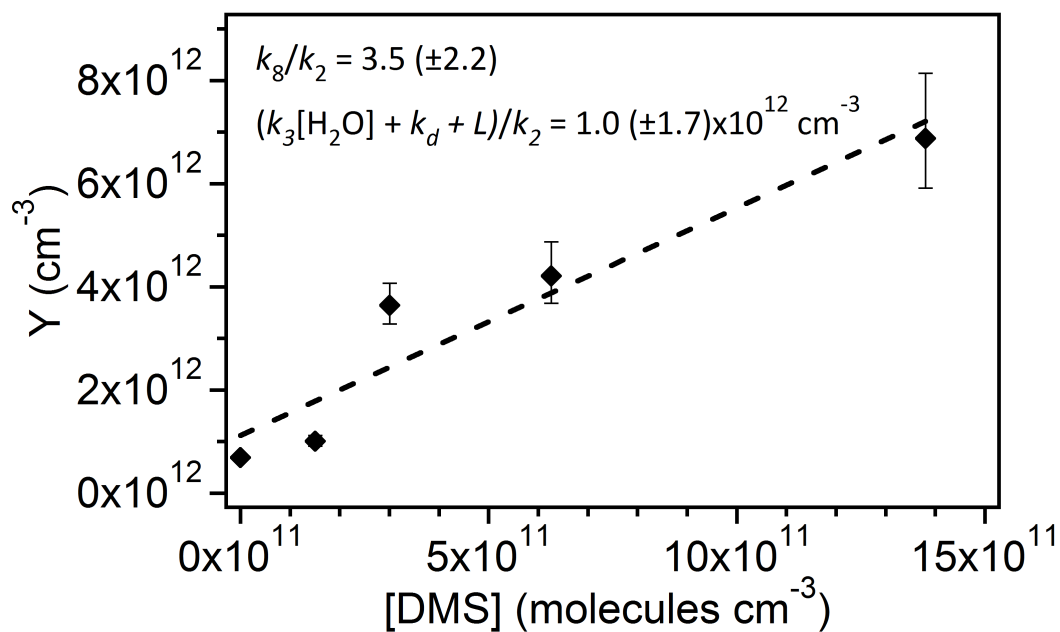
14

15

16

17

18



- 1
- 2 Figure 6. Application of Equation E8 to derive rate constants for reaction of ISOP-SCI with
- 3 DMS ( $k_8$ ) relative to that for reaction with  $\text{SO}_2$ .  $Y = [\text{SO}_2]((1/f)-1) - k_9[\text{acid}]/k_2$ .